Lattice calculation of electric dipole moments and form factors of the nucleon

M. Abramczyk
Physics Department, University of Connecticut, Storrs, Connecticut 06269, USA

S. Aoki
Center for Gravitational Physics, Yukawa Institute for Theoretical Physics, Kyoto University, Kyoto 606-8502, Japan and Center for Computational Sciences, University of Tsukuba, Tsukuba 305-8577, Japan

T. Blum
Physics Department, University of Connecticut, Storrs, Connecticut 06269, USA and RIKEN/BNL Research Center, Brookhaven National Laboratory, Upton, New York 11973, USA

T. Izubuchi
Physics Department, Brookhaven National Laboratory, Upton, New York 11973, USA and RIKEN/BNL Research Center, Brookhaven National Laboratory, Upton, New York 11973, USA

H. Ohki
RIKEN/BNL Research Center, Brookhaven National Laboratory, Upton, New York 11973, USA

S. Syritsyn[*]
Jefferson Lab, 12000 Jefferson Ave, Newport News, Virginia 23606, USA; Kavli Institute for Theoretical Physics, UC Santa Barbara, California 93106, USA; Department of Physics and Astronomy, Stony Brook University, Stony Brook, New York 11794, USA; and RIKEN/BNL Research Center, Brookhaven National Laboratory, Upton, New York 11973, USA

(Received 8 March 2017; published 10 July 2017)

We analyze commonly used expressions for computing the nucleon electric dipole form factors (EDFF) F_3 and moments (EDM) on a lattice and find that they lead to spurious contributions from the Pauli form factor F_2 due to inadequate definition of these form factors when parity mixing of lattice nucleon fields is involved. Using chirally symmetric domain wall fermions, we calculate the proton and the neutron EDFF induced by the CP-violating quark chromo-EDM interaction using the corrected expression. In addition, we calculate the electric dipole moment of the neutron using a background electric field that respects time translation invariance and boundary conditions, and we find that it decidedly agrees with the new formula but not the old formula for F_3. Finally, we analyze some selected lattice results for the nucleon EDM and observe that after the correction is applied, they either agree with zero or are substantially reduced in magnitude, thus reconciling their difference from phenomenological estimates of the nucleon EDM.

DOI: 10.1103/PhysRevD.96.014501

I. INTRODUCTION

The origin of nuclear matter can be traced back to the excess of nucleons over antinucleons in the early Universe, and it is one of the greatest puzzles in physics, known as the baryonic asymmetry of the Universe (BAU). One of the required conditions for the BAU is violation of the CP symmetry ($\not{CP}$). In the standard model (SM), the CKM matrix phases lead to CP violations in weak interactions, but their magnitudes are not sufficient to explain the BAU, and signs of additional $\not{CP}$ are actively sought in experiments. The most promising ways to look for $\not{CP}$ are measurements of electric dipole moments (EDM) of atoms, nucleons and nuclei. In particular, the standard-model prediction for the neutron EDM is 5 orders below the current experimental bound, and represents a negligible background. Near-future EDM experiments plan to improve this bound by 2 orders of magnitude, and are capable of constraining various beyond-the-standard-model (BSM) extensions of particle physics, purely from low-energy nuclear and atomic high-precision experiments. Knowledge of nucleon structure and interactions is necessary to interpret these experiments in terms of quark and

[*]Corresponding author.
sergey.syritsyn@stonybrook.edu

gluon effective operators and to put constraints on proposed extensions of the standard model, in particular SUSY and GUT models, as sources of additional $\not{CP}$. Connecting the quark- and gluon-level to hadron-level effective $\not{CP}$ interactions is an urgent task for lattice QCD (an extensive review of EDM phenomenology can be found in Ref. [1]).

The proton and the neutron can have electric dipole moments only if the symmetry is broken by P- or T-odd interactions. The only such dimension-4 operator is the QCD $\bar{\theta}$ angle ($\bar{\theta}$ stands for the physically relevant combination of the QCD θ angle and quark mass phases). The $\bar{\theta}$-induced nucleon EDMs (nEDMs) have been calculated on a lattice from energy shifts in a uniform background electric field [2–4] or by extracting the P-odd electric dipole form factor (EDFF) $F_3(Q^2)$ from nucleon matrix elements of the quark vector current in a $\not{CP}$ vacuum [5–11]. Nucleon EDMs have also been studied using QCD sum rules, quark models, and chiral perturbation theory (see Refs. [12–18]). On a lattice, quark EDM-induced nucleon EDMs have been recently computed in a partially quenched framework [19]. Another important dimension-5 (or 6)[1] operator is the CP-odd quark-gluon interaction, also known as the chromo-electric dipole moment (cEDM):

$$\mathcal{L}_{\mathrm{cEDM}} = i \sum_{\psi=u,d} \frac{\tilde{\delta}_\psi}{2} \bar{\psi}(T^a G^a_{\mu\nu})\sigma^{\mu\nu}\gamma_5\psi, \tag{1}$$

and calculations of cEDM-induced nEDMs have recently been started using Wilson fermions [20,21].

In this paper, we report several important achievements in studying nucleon EDMs on a lattice. First, we argue that the commonly accepted methodology for computing electric dipole form factors of spin-1/2 particles on a lattice identifies the electric dipole moment form factor incorrectly. In particular, in the standard analysis of the nucleon-current correlators [5–11], the electric dipole form factor F_3 receives a large and likely dominant contribution from spurious mixing with the Pauli form factor F_2. The energy-shift methods [2–4] are not affected by such mixing, but their precision has not been sufficient to detect the discrepancy. This problem affects all of the previous lattice calculations of the nucleon EDFFs and EDMs that use nucleon-current correlators, including those studying the $\bar{\theta}$ angle [5–10] as well as the more recent ones studying the quark chromo-EDM [20,21]. We demonstrate the problem formally in Sec. II and also derive the correction for the results of Refs. [5–11] to subtract the spurious mixing with F_2. In addition, in Sec. II C we study the energy shift of a neutral particle on a Euclidean lattice in a uniform background electric field. We introduce the uniform electric field, preserving translational invariance and periodic boundary conditions on a lattice [22]. In order to satisfy these conditions, the electric field has to be analytically continued to an imaginary value upon the Wick rotation from Minkowski to Euclidean spacetime, and we demonstrate that the eigenstates of a fermion possessing an EDM are shifted by a purely imaginary value. In Sec. III C, we apply this formalism to the analysis of neutron correlators computed in the presence of the quark chromo-EDM interaction (1).

Calculations of the neutron EDM in background fields are independent from parity-mixing ambiguities, and this allows us to validate our new formula for the EDFF F_3 numerically. The difference is evident only if the nucleon "parity-mixing" angle α_5 is large, $\alpha_5 \gtrsim 1$. Quark chromo-EDMs generate very strong parity mixing compared to the $\bar{\theta}$ angle, which is beneficial for our numerical check. In Sec. III B, we calculate the proton and neutron EDFFs $F_{3p,n}(Q^2)$ induced by the quark chromo-EDM interaction (1), as well as the regular CP-even Dirac and Pauli form factors $F_{1,2}$. In Sec. III D, we compare the EDM results from the form-factor and the energy-shift calculations, providing a numerical confirmation of the validity of our new EDFF analysis. Finally, in Sec. IV we analyze some select results for the nucleon EDM induced by the $\bar{\theta}$ angle available in the literature [5,6,8,10,11] and attempt to correct them according to our findings.

II. CP-ODD FORM FACTORS OF SPIN-1/2 PARTICLES

A. Form factors and parity mixing

In this section, we argue that the ubiquitously used expression for computing the CP-odd electric dipole form factor F_3 *on a lattice* does not correspond to the electric dipole moment measured in experiments and leads to a finite and perhaps dominant contribution from the Pauli form factor F_2 to the reported values of EDFF F_3 and the EDM of the proton and the neutron. First, we recall the lattice framework for the calculation of the CP-violating form factor F_3 first introduced in Ref. [5], and later used without substantial changes in the subsequent papers studying the QCD θ term [6–11], as well as more recent papers studying the quark chromo-EDM [20,21].

To compute nucleon form factors on a lattice, one evaluates nucleon two- and three-point functions (see Fig. 1) in the presence of CP-violating ($\not{CP}$) interactions:

$$C^{\not{CP}}_{N\bar{N}}(\vec{p},t) = \sum_{\vec{x}} e^{-i\vec{p}\cdot\vec{x}} \langle N(\vec{x},t)\bar{N}(0)\rangle_{\not{CP}}, \tag{2}$$

$$C^{\not{CP}}_{NJ\bar{N}}(\vec{p}',t_{\mathrm{sep}};\vec{q},t_{\mathrm{op}}) = \sum_{\vec{y},\vec{z}} e^{-i\vec{p}'\cdot\vec{y}+i\vec{q}\cdot\vec{z}} \langle N(\vec{y},t_{\mathrm{sep}}) J^\mu(\vec{z},t_{\mathrm{op}}) \bar{N}(0)\rangle_{\not{CP}}. \tag{3}$$

The subscript $\not{CP}$ indicates that these correlation functions are evaluated in a $\not{CP}$ vacuum, either with a finite value of

[1] These operators are sometimes referred to as "dimension-6" because they contain a factor of the Higgs field in the standard model.

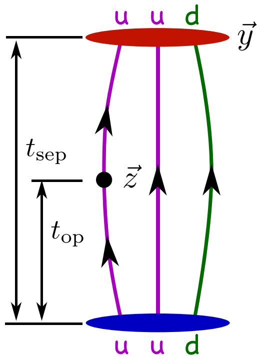

FIG. 1. Nucleon *connected* three-point function [Eq. (3)] and labeling of the source-sink separation $t_{\rm sep}$ and operator insertion time $t_{\rm op}$.

the relevant $\mathcal{CP}$ coupling or an infinitesimal value, i.e. performing first-order Taylor expansion of the correlation functions. As argued in Ref. [5], as well as earlier model calculations [14,15], the $\mathcal{CP}$ background leads to a $\mathcal{CP}$ phase in the nucleon mass in the Dirac equation that governs the on-shell nucleon fields N, $\bar{N}$:

$$(i\partial\!\!\!/ - m_{N'}e^{-2i\alpha_5\gamma_5})N(x) = 0, \tag{4}$$

where the real-valued $m_{N'} > 0$ is the nucleon ground-state mass in the new vacuum. The spinor wave functions $\tilde{u}_p$, $\bar{\tilde{u}}_p$ for the new ground states

$$\langle\Omega|N|p,\sigma\rangle_{\mathcal{CP}} = Z_{N'}\tilde{u}_{p,\sigma} = Z_{N'}e^{i\alpha_5\gamma_5}u_{p,\sigma} \tag{5}$$

also satisfy the same Dirac equation:

$$(p\!\!\!/ - m_{N'}e^{-2i\alpha_5\gamma_5})\tilde{u}_p = (p\!\!\!/ - m_{N'}e^{-2i\alpha_5\gamma_5})e^{i\alpha_5\gamma_5}u_p = 0, \tag{6}$$

where the chirally rotated spinors $\tilde{u}_p$, $\bar{\tilde{u}}_p$ have the Lorentz-invariant $\mathcal{CP}$ phase similar to the mass term,

$$\tilde{u} = e^{i\alpha_5\gamma_5}u, \qquad \bar{\tilde{u}} = \bar{u}e^{i\alpha_5\gamma_5}, \tag{7}$$

while the regular spinors u_p, $\bar{u}_p$ satisfy the regular Dirac equation with a real-valued nucleon mass,

$$(p\!\!\!/ - m_{N'})u_p = 0, \qquad \bar{u}_p(p\!\!\!/ - m_{N'}) = 0. \tag{8}$$

From the above equation (8), it also follows that the spinors u_p, $\bar{u}_p$ transform under spatial reflection (parity P) as the regular spinors:

$$\gamma_4 u_{p=(\vec{p},E)} = u_{\tilde{p}=(-\vec{p},E)}. \tag{9}$$

Below we will discuss correlation functions on a Euclidean lattice, which depend on Wick-rotated four-momenta and are more conveniently expressed using the Euclidean matrices $[\gamma^\mu]_{\mathcal{E}uc}$ (A4). Whenever a confusion may arise, we will explicitly specify the type $\mathcal{M}2$ (Minknowski) or $\mathcal{E}uc$ (Euclidean) of γ-matrices and four-vectors (see Appendix A for details). The Euclidean versions of the Dirac equation (8) for the nucleon spinors are

$$(ip\!\!\!/_{\mathcal{E}uc} + m_{N'})u_p = 0, \qquad \bar{u}_p(ip\!\!\!/_{\mathcal{E}uc} + m_{N'}) = 0, \tag{10}$$

where $(-ip\!\!\!/_{\mathcal{E}uc}) = (-i)p^\mu_{\mathcal{E}uc}[\gamma_\mu]_{\mathcal{E}uc} = E[\gamma^4]_{\mathcal{E}uc} - i\vec{p}\cdot[\vec{\gamma}]_{\mathcal{E}uc}$, in which the Euclidean on-shell four-momentum $p^\mu_{\mathcal{E}uc} = (\vec{p}, iE)$ is contracted with the Euclidean γ-matrices, and $E = \sqrt{m^2_{N'} + \vec{p}'^2}$ is the real-valued on-shell energy of the nucleon. Due to the chiral phase (7), the nucleon propagator on a lattice (2) contains chiral phases $e^{i\alpha_5\gamma_5}$. Keeping only the ground state and omitting the exponential time dependence for simplicity, we get

$$\begin{aligned} C_{N\bar{N}}(\vec{p},t)|_{g.s.} &\propto \frac{\sum_\sigma \tilde{u}_{p,\sigma}\bar{\tilde{u}}_{p,\sigma}}{2E_{N'}} = \frac{-ip\!\!\!/_{\mathcal{E}uc} + m_{N'}e^{2i\alpha_5\gamma_5}}{2E_{N'}} \\ &= e^{i\alpha_5\gamma_5}\frac{-ip\!\!\!/_{\mathcal{E}uc} + m_{N'}}{2E_{N'}}e^{i\alpha_5\gamma_5}. \end{aligned} \tag{11}$$

Analogously, the expression for the nucleon-current correlator (3) contains the phases $e^{i\alpha_5\gamma_5}$:

$$\begin{aligned} &C_{NJ\bar{N}}(\vec{p}', t_{\rm sep}; \vec{q}, t_{\rm op})|_{g.s.} \\ &\quad\propto \sum_{\sigma',\sigma}\tilde{u}_{p',\sigma'}\langle p',\sigma'|J^\mu|p,\sigma\rangle_{\mathcal{CP}}\bar{\tilde{u}}_{p,\sigma} \\ &\quad= e^{i\alpha_5\gamma_5}\left(\sum_{\sigma',\sigma}u_{p',\sigma'}\langle p',\sigma'|J^\mu|p,\sigma\rangle_{\mathcal{CP}}\bar{u}_{p,\sigma}\right)e^{i\alpha_5\gamma_5}. \end{aligned} \tag{12}$$

The problem with the commonly used expression for the three-point function is caused by unclear physical interpretation of a parity-mixed fermion state (5) on a lattice. In Refs. [5–11], the nucleon matrix elements of the vector current in a $\mathcal{CP}$ vacuum are assumed to have the form (in Minkowski space, up to sign conventions for F_3 and F_A)

$$\begin{aligned} &\langle p',\sigma'|J^\mu|p,\sigma\rangle_{\mathcal{CP}} \\ &\quad\stackrel{?}{=}\bar{\tilde{u}}_{p',\sigma'}\left[F_1(Q^2)\gamma^\mu + \tilde{F}_2(Q^2)\frac{i\sigma^{\mu\nu}q_\nu}{2m_{N'}}\right. \\ &\qquad\left. - \tilde{F}_3(Q^2)\frac{\gamma_5\sigma^{\mu\nu}q_\nu}{2m_{N'}} + F_A(Q^2)\frac{(q\!\!\!/q^\mu - \gamma^\mu q^2)\gamma_5}{m^2_{N'}}\right]\tilde{u}_{p,\sigma}, \end{aligned} \tag{13}$$

where $q = p' - p$, $Q^2 = -[q^2]_{\mathcal{M}2} = -(q^4)^2 + \vec{q}^2$, F_1 and $\tilde{F}_2$ are the Dirac and Pauli form factors, $\tilde{F}_3$ is the electric dipole form factor (EDFF), and F_A is the anapole form factor (notations $\tilde{F}_{2,3}$ are introduced to avoid confusion with the true $F_{2,3}$ below). The matrix element expression (13), however, disagrees with the literature [23],

$$\begin{aligned}\langle p',\sigma'|J^\mu|p,\sigma\rangle_{\not{CP}} &= \bar{u}_{p',\sigma'}\left[F_1(Q^2)\gamma^\mu + F_2(Q^2)\frac{i\sigma^{\mu\nu}q_\nu}{2m_{N'}}\right. \\ &\left. - F_3(Q^2)\frac{\gamma_5\sigma^{\mu\nu}q_\nu}{2m_{N'}} + F_A(Q^2)\frac{(\not{q}q^\mu - \gamma^\mu q^2)\gamma_5}{m_{N'}^2}\right]u_{p,\sigma}, \end{aligned} \tag{14}$$

in which the vertex spin matrix

$$\begin{aligned}\Gamma^\mu(p',p) &= F_1\gamma^\mu + (F_2 + iF_3\gamma_5)\frac{i\sigma^{\mu\nu}q_\nu}{2m_{N'}} \\ &+ F_A\frac{(\not{q}q^\mu - \gamma^\mu q^2)\gamma_5}{m_{N'}^2}\end{aligned} \tag{15}$$

is contracted with the spinors satisfying the regular parity transformations (9). Only in this case, the contribution of the form factor F_3 to the matrix element $\langle p',\sigma'|J^\mu|p,\sigma\rangle$ transforms as an axial four-vector so that F_3 is indeed the P-, CP-odd coupling of the nucleon to the electromagnetic potential [23]. Let us show that this is not the case if the matrix element of the current has the form (13). Upon spatial reflection, the true four-vectors of momenta and current transform as

$$(\vec{p}^{(\prime)}, p^{4(\prime)}) \to (-\vec{p}^{(\prime)}, p^{4(\prime)}), (\vec{J}, J^4) \to (-\vec{J}, J^4), \tag{16}$$

while the axial vector current A^μ transforms with the sign opposite to J^μ:

$$(\vec{A}, A^4) \to (\vec{A}, -A^4). \tag{17}$$

The chirally rotated spinors transform as

$$\tilde{u}_{\vec{p}} \to \tilde{u}_{-\vec{p}} = e^{2i\alpha_5\gamma_5}\gamma_4\tilde{u}_{\vec{p}}, \tag{18}$$

$$\bar{\tilde{u}}_{\vec{p}} \to \bar{\tilde{u}}_{-\vec{p}} = \bar{\tilde{u}}_{\vec{p}}\gamma_4 e^{2i\alpha_5\gamma_5}, \tag{19}$$

up to an irrelevant overall phase factor. Finally, remembering that the spatial momentum $\vec{q}$ is also reflected and using the identities

$$\gamma_4\sigma^{i\nu}(-\vec{q}, q^4)_\nu\gamma_4 = -\sigma^{i\nu}(\vec{q}, q^4)_\nu, \tag{20}$$

$$\gamma_4\sigma^{4\nu}(-\vec{q}, q^4)_\nu\gamma_4 = \sigma^{4\nu}(\vec{q}, q^4)_\nu, \tag{21}$$

we observe that the combination of the $\tilde{F}_{2,3}$ form factors transforms as

$$e^{2i\alpha_5}(\tilde{F}_2 + i\tilde{F}_3) \to e^{-2i\alpha_5}(\tilde{F}_2 - i\tilde{F}_3). \tag{22}$$

Therefore, we conclude that the axial-vector contribution of the matrix element (13) appears because of the parity-odd form-factor combination

$$\mathrm{Im}[e^{2i\alpha_5}(\tilde{F}_2 + i\tilde{F}_3)] = \sin(2\alpha_5)\tilde{F}_2 + \cos(2\alpha_5)\tilde{F}_3, \tag{23}$$

which is different from F_3 if $\alpha_5 \neq \pi n$.

Since the expression (13) is used in lattice calculations so ubiquitously, we present extensive arguments that it is not correct. The form factor F_A is irrelevant for this discussion, and will be omitted.[2] In Appendix B, we directly show that it is the expression (14) that leads to the correct CP-odd EDM coupling $\propto \vec{E}\cdot\vec{S}$, and the forward limits $Q^2 \to 0$ of the form factors $F_2(Q^2)$ and $F_3(Q^2)$ yield the anomalous magnetic κ and electric ζ dipole moments [in units $e/(2m_N)$], respectively. In Sec. II B, we calculate the mass shift of a particle governed by the Dirac equation with a chirally rotated mass in the background electric field.

In this section, we offer several heuristic arguments why expression (13) is not correct. First, revisiting the form-factor expressions (13) and (14), we note that the only effect of the chiral phases is to mix form factors F_2 and F_3 into each other,

$$\begin{aligned}&\bar{\tilde{u}}_{p'}\left[F_1\gamma^\mu + (\tilde{F}_2 + i\tilde{F}_3\gamma_5)\frac{i\sigma^{\mu\nu}q_\nu}{2m_{N'}}\right]\tilde{u}_p \\ &= \bar{u}_{p'}\left[F_1\gamma^\mu + e^{2i\alpha_5\gamma_5}(\tilde{F}_2 + i\tilde{F}_3\gamma_5)\frac{i\sigma^{\mu\nu}q_\nu}{2m_{N'}}\right]u_p,\end{aligned} \tag{24}$$

while the form factor F_1, as well as the omitted F_A, are independent of α_5. Thus, the form factors $\tilde{F}_{2,3}$ computed in Refs. [5–11] are linear combinations of the true form factors $F_{2,3}$:

$$\begin{aligned}&(F_2 + iF_3\gamma_5) = e^{2i\alpha_5\gamma_5}(\tilde{F}_2 + i\tilde{F}_3\gamma_5), \quad \text{or} \\ &\begin{cases}\tilde{F}_2 = \cos(2\alpha_5)F_2 + \sin(2\alpha_5)F_3, \\ \tilde{F}_3 = -\sin(2\alpha_5)F_2 + \cos(2\alpha_5)F_3,\end{cases}\end{aligned} \tag{25}$$

which is also consistent with Eq. (23).

It is easy to see that the effect of the phase $e^{i\alpha_5\gamma_5}$ can be completely removed by a field redefinition $N' = e^{-i\alpha_5\gamma_5}N$. After this transformation, the on-shell nucleon field N' will satisfy the Dirac equation with a real-valued mass $m_{N'}$,

$$(i\not{\partial} - m_{N'})N'(x) = 0. \tag{26}$$

A similar transformation for the nucleon correlators $C_{N[J]\bar{N}} \to C'_{N[J]\bar{N}} = e^{-i\alpha_5\gamma_5}C_{N[J]\bar{N}}e^{-i\alpha_5\gamma_5}$ will remove any dependence on α_5 altogether. Note, however, that this is the case only if Eq. (14) is used for the nucleon matrix elements of the current. Thus, this phase is purely conventional and similar to the operator normalization $Z_{N'}$, in that physical quantities cannot depend on it. In lattice calculations, however, this phase is not known in advance and

[2] It is also worth noting that F_A is not affected by the parity mixing, unlike $F_{2,3}$.

must be determined numerically to be removed from the two- and three-point correlators [Eqs. (2) and (3)].

To make this point more evident, suppose one calculated nucleon form factors in CP-even QCD, but using unconventional nucleon interpolating fields $e^{i\alpha_5'\gamma_5}N$ with some arbitrary phase α_5'. If Eq. (13) were used, the definition of $\tilde{F}_{2,3}$ would depend on this arbitrarily chosen α_5'. Consequently, because of the spurious mixing (25), the electric dipole form factor would obtain the nonzero value $\tilde{F}_3 = -F_2\sin(2\alpha_5')$ in absence of any $\not{C}\not{P}$ interactions. Analogously, the apparent nucleon magnetic moment $\tilde{\mu}_{N'} = \tilde{G}_M(0) = F_1(0) + \tilde{F}_2$ would have contributions from both F_2 and F_3. In a CP-even QCD vacuum, $F_3 = 0$ and the mixing (25) would just reduce the contribution of F_2 to $\tilde{\mu}_{N'}$ by a factor of $\cos(2\alpha_5')$. This would happen because the spin operator $\Sigma^k = \frac{1}{2}\epsilon^{ijk}\sigma^{ij}$ was "sandwiched" between chirally rotated 4-spinors and

$$(2\vec{S})^k = \Sigma^k = \bar{\tilde{u}}_{p'}\frac{\Sigma^k}{2m_{N'}}\tilde{u}_p = \xi'^{\dagger}\sigma^k\xi\cos(2\alpha_5), \tag{27}$$

where the initial and final momenta $\vec{p}$, $\vec{p}' \approx 0$ and ξ, ξ' are the corresponding 2-spinors.

The resolution to this apparent paradox is hinted at by the modified form of the Gordon identity for the spinors $\tilde{u}_p$, $\bar{\tilde{u}}_p$. Since these spinors satisfy the Dirac equation with the chirally rotated mass (6), the Gordon identity takes the form

$$\bar{\tilde{u}}_{p'}\gamma^\mu\tilde{u}_p = \bar{\tilde{u}}_{p'}\left[\frac{(p'+p)^\mu + i\sigma^{\mu\nu}(p'-p)_\nu}{2m_{N'}e^{2i\alpha_5\gamma_5}}\right]\tilde{u}_p, \tag{28}$$

which is obtained from the standard Gordon identity by replacing $m_{N'} \to m_{N'}e^{2i\alpha_5\gamma_5}$. The form of the nucleon-current vertex must be compatible with the Gordon identity, which relates form factors $F_{1,2}$ to G_M. Therefore, to make the nucleon-current vertex compatible with the spinors $\tilde{u}_p$, $\bar{\tilde{u}}_p$, the nucleon mass in the $\tilde{F}_{2,3}$ terms in Eq. (13) has to be adjusted similarly to Eq. (28), which leads back to the correct expression (14).

Finally, we emphasize that Eqs. (13) and (14) result in different prescriptions for analyzing the three-point nucleon-current correlators:

$$\begin{aligned} &C_{NJ\bar{N}}(\vec{p}, t_{\mathrm{sep}}; \vec{q}, t_{\mathrm{op}})|_{g.s.} \\ &\overset{?}{=} e^{-E'_{N'}(t_{\mathrm{sep}}-t_{\mathrm{op}})-E_{N'}t_{\mathrm{op}}}e^{i\alpha_5\gamma_5} \\ &\quad\times\frac{-i\not{p}'_{\mathcal{E}uc}+m_{N'}}{2E'_{N'}}\{e^{i\alpha_5\gamma_5}\}^?\Gamma^\mu_{\mathcal{E}uc}\{e^{i\alpha_5\gamma_5}\}^? \\ &\quad\times\frac{-i\not{p}_{\mathcal{E}uc}+m_{N'}}{2E_{N'}}e^{i\alpha_5\gamma_5}, \end{aligned} \tag{29}$$

where phase factors in curly braces $\{e^{i\alpha_5\gamma_5}\}^?$ are present only if one uses the (incorrect) Eq. (13). In the above equation, we have introduced the Euclidean nucleon-current vertex

$$\Gamma^\mu_{\mathcal{E}uc}(p',p) = \left[F_1\gamma^\mu + (F_2 + i\gamma_5F_3)\frac{\sigma^{\mu\nu}q_\nu}{2m_{N'}}\right]_{\mathcal{E}uc}. \tag{30}$$

B. EDM energy shift from Dirac equation

We argued in the previous section that one has to use the regular "even" spinors satisfying Eq. (9) to evaluate the nucleon matrix elements even if the QCD vacuum is CP-broken, contrary to the previous works [5–11]. Most of the ambiguity must have resulted from the notion that in a CP-broken vacuum, particles are no longer parity eigenstates; hence, the argument goes, the nucleon must be described by a parity-mixed spinor. This argument is rather confusing, because parity transformations of fermion fields are fixed only up to a phase factor, and only a fermion-antifermion pair may have definite parity. To clarify this question, in this section we calculate the energy spectrum of a particle described by the Dirac operator $\tilde{\not{D}}_N$ with the complex mass $me^{-2i\alpha_5\gamma_5}$ and with magnetic and electric dipole interactions in the form (13) in the background of uniform magnetic and electric fields. Such an operator is exactly the nucleon effective operator on a lattice. The zero modes of this operator (i.e., the poles of its Green's function) must correspond to particle eigenstates, and their calculation avoids the spinor phase ambiguity completely. The energy shifts linear in these fields may then be identified with the magnetic κ and electric ζ dipole moments, respectively.

The effective action for the Euclidean lattice nucleon field in the $\not{C}\not{P}$ vacuum and pointlike electromagnetic interaction introduced via a "long derivative" is

$$\mathcal{L}_{\mathrm{int}} = \bar{N}(i\not{\partial} - Q\gamma^\mu A_\mu - me^{-2i\alpha_5\gamma_5})N, \tag{31}$$

where we neglect the momentum-transfer dependence of the nucleon form factors for simplicity, setting F_1 to a "pointlike" value $Q = F_1(0) = \mathrm{const}$. In the absence of electromagnetic potential A_μ, the nucleon propagator $\langle N\bar{N}\rangle$ takes the form (11). We add effective pointlike anomalous magnetic $\tilde{\kappa} = \tilde{F}_2(0)$ and electric $\tilde{\zeta} = \tilde{F}_3(0)$ dipole interactions to the interaction vertex:

$$Q\gamma^\mu \to Q\gamma^\mu + \tilde{\kappa}\frac{i\sigma^{\mu\nu}q_\nu}{2m} - \tilde{\zeta}\frac{\gamma_5\sigma^{\mu\nu}q_\nu}{2m}. \tag{32}$$

Using conventions (B10)–(B12) as well as (B8) and (B9), the Dirac equation for N becomes

$$\left[\not{p} - Q\gamma^\mu A_\mu - (\tilde{\kappa} + i\tilde{\zeta}\gamma_5)\frac{1}{2}F_{\mu\nu}\frac{\sigma^{\mu\nu}}{2m} - me^{-2i\alpha_5\gamma_5}\right]N = 0. \tag{33}$$

We are going to find the energy levels of the particle in the presence of constant field strength $F_{\mu\nu}$. To avoid irrelevant complications, we consider only a neutral particle with $Q = 0$. Using the identity (A3) to trade γ_5 for $F_{\mu\nu} \to \tilde{F}_{\mu\nu}$, we obtain the Dirac operator in the block-diagonal form in the chiral basis (A1):

$$\not{p} - \frac{1}{2}(\tilde{\kappa} F_{\mu\nu} - \tilde{\zeta}\tilde{F}_{\mu\nu})\frac{\sigma^{\mu\nu}}{2m} - me^{-2i\alpha_5\gamma_5} = \begin{pmatrix} -M & E - \vec{p}\cdot\vec{\sigma} \\ E + \vec{p}\cdot\vec{\sigma} & -M^\dagger \end{pmatrix}, \tag{34}$$

where $M = me^{2i\alpha_5} - \frac{1}{2m}(\tilde{\kappa} - i\tilde{\zeta})(\vec{H} + i\vec{E})\cdot\vec{\sigma}$. In the rest frame, $\vec{p} = (\vec{0}, E_0)$, and the operator (34) has solutions if

$$\det\begin{pmatrix} -M & E_0 \\ E_0 & -M^\dagger \end{pmatrix} = 0 \Leftrightarrow \det(E_0^2 - M^\dagger M) = \det(E_0^2 - MM^\dagger) = 0. \tag{35}$$

Up to terms linear in $\tilde{\kappa}$, $\tilde{\zeta}$, the normal operator $M^\dagger M$ is

$$\begin{aligned} M^\dagger M &= m^2 - \frac{1}{2}[e^{2i\alpha_5}(\tilde{\kappa} + i\tilde{\zeta})(\vec{H} - i\vec{E}) \\ &\quad + e^{-2i\alpha_5}(\tilde{\kappa} - i\tilde{\zeta})(\vec{H} + i\vec{E})]\cdot\vec{\sigma} + O(\tilde{\kappa}^2, \tilde{\zeta}^2) \\ &= m^2 - [\kappa\vec{H} + \zeta\vec{E}]\cdot\vec{\sigma} + O(\kappa^2, \zeta^2), \end{aligned} \tag{36}$$

where in the last line we have redefined $e^{2i\alpha_5}(\tilde{\kappa} + i\tilde{\zeta}) = (\kappa + i\zeta)$, which is the same transformation as Eq. (25). Finally, the energy of the particle's interaction with the EM background is

$$E_0 - m = -\frac{\kappa}{2m}\vec{H}\cdot\hat{\Sigma} - \frac{\zeta}{2m}\vec{E}\cdot\hat{\Sigma} + O(\kappa^2, \zeta^2), \tag{37}$$

where $\hat{\Sigma}$ is the unit vector of the particle's spin. From the interaction energy, we conclude that indeed

$$\kappa = F_2(0), \qquad \zeta = F_3(0) \tag{38}$$

are the particle's magnetic and electric dipole moments. For a neutral particle such as the neutron, the form factor $F_2(0)$ is indeed the full magnetic moment.

Thus, we have shown that if the field of a spin-1/2 particle is governed by the Dirac equation with a complex mass (33), electric and magnetic dipole moments have to be properly adjusted $(\tilde{\kappa}, \tilde{\zeta}) \to (\kappa, \zeta)$. This adjustment is equivalent to the redefinition of the field and the operator

$$\begin{aligned} N &\to N' = e^{-i\alpha_5\gamma_5}N, \\ \tilde{\not{D}}_N &\to \not{D}_N = e^{i\alpha_5\gamma_5}\tilde{\not{D}}_N e^{i\alpha_5\gamma_5} \end{aligned} \tag{39}$$

to remove the complex (chiral) phase from the mass, where $\tilde{\not{D}}_N$ and $\not{D}_N$ contain $\tilde{\kappa}$, $\tilde{\zeta}$ and κ, ζ, respectively.

C. EDM energy shift in Euclidean spacetime

In order to verify our findings, in this paper we calculate the EDM of the neutron on a lattice using two methods: (1) from the energy shift in the background electric field, and (2) using the new formula for the CP-odd form factor F_3. The electric field is introduced following Ref. [22] and preserving the antiperiodic boundary condition in time. Such an electric field [22] is analytically continued to an imaginary value. If the particle's electric dipole moment is finite and real-valued, the energy shift is imaginary, which might be problematic for the analysis of corresponding lattice correlators. However, in our methodology, the CP-odd interaction is always infinitesimal, and so are the electric dipole moments and the corresponding energy shifts, which are extracted from Taylor expansion of the nucleon correlation functions to the first order in the CP-odd interaction. In this paper, we study only neutral particles, because the analysis of charged particle propagators is more complicated [24].

In this section, we repeat the calculation of Sec. II B for a neutral particle on a Euclidean lattice, which has on-shell Euclidean four-momentum $p_{\mathcal{E}uc} = (\vec{p}, iE)$, with energy $E = \sqrt{E_0^2 + \vec{p}^2}$ up to discretization errors. The energy at rest E_0 is modified from the mass m due to electric and magnetic dipole interactions. To avoid any confusion, we imply no relation between the Minkowski $\vec{E}$, $\vec{H}$ and Euclidean $\vec{\mathcal{E}}$, $\vec{\mathcal{H}}$ electric and magnetic fields. Instead, we introduce *ad hoc* uniform Abelian fields on a lattice (see Fig. 2) preserving boundary conditions in both space and time [22] that probe the MDM and EDM: the magnetic $\epsilon^{ijk}\mathcal{H}^k = (\partial_i\mathcal{A}_j - \partial_j\mathcal{A}_i) = n_{ij}\Phi_{ij}$ (no summation over i, j)

$$\begin{cases} \mathcal{A}_{x,j} & = n_{ij}\Phi_{ij}x_i \\ \mathcal{A}_{x,i}|_{x_i=L_i-1} & = -n_{ij}\Phi_{ij}L_i x_j \end{cases} \tag{40}$$

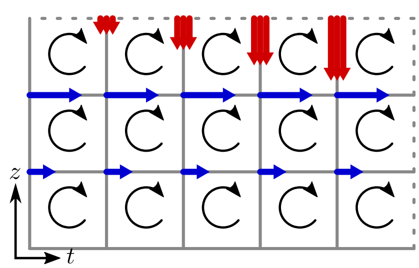

FIG. 2. Abelian gauge potential (41) corresponding to a uniform background electric field on a periodic lattice [22]. The horizontal arrows show positive, and the triple vertical arrows show negative Abelian potential $\propto L_z$ on the corresponding lattice links. The resulting circulation of the Abelian potential is the same around each plaquette (shown by the black arrows) and equal to the flux of the electric field $\frac{2\pi}{L_z L_t}$.

and the electric $\mathcal{E}^k = (\partial_k \mathcal{A}_4 - \partial_4 \mathcal{A}_k) = n_{k4}\Phi_{k4}$

$$\begin{cases} \mathcal{A}_{x,4} & = n_{k4}\Phi_{k4}x_k \\ \mathcal{A}_{x,k}|_{x_k=L_k-1} & = -n_{k4}\Phi_{k4}L_k x_4 \end{cases}, \tag{41}$$

where $\Phi_{\mu\nu} = \frac{6\pi}{L_\mu L_\nu}$ is the quantum of field flux through a plaquette $(\mu\nu)$ and $n_{\mu\nu}$ is the corresponding number of quanta. The fractional quark charges $Q_u = 2/3$, $Q_d = -1/3$ and the periodic boundary conditions require that the flux through the edge of the lattice $L_\mu L_\nu \Phi_{\mu\nu} = 6\pi$. From potentials (40) and (41), the Euclidean field strength tensor $\mathcal{F}_{\mu\nu} = \partial_\mu \mathcal{A}_\nu - \partial_\nu \mathcal{A}_\mu$:

$$\mathcal{F}_{\mu\nu} = \begin{array}{cc} & \begin{array}{cccc} 1 & 2 & 3 & 4 \end{array} \\ \begin{array}{c} 1 \\ 2 \\ 3 \\ 4 \end{array} & \begin{pmatrix} 0 & \mathcal{H}^3 & -\mathcal{H}^2 & \mathcal{E}^1 \\ -\mathcal{H}^3 & 0 & \mathcal{H}^1 & \mathcal{E}^2 \\ \mathcal{H}^2 & -\mathcal{H}^1 & 0 & \mathcal{E}^3 \\ -\mathcal{E}^1 & -\mathcal{E}^2 & -\mathcal{E}^3 & 0 \end{pmatrix} \end{array}, \tag{42}$$

with $\vec{\mathcal{H}} = (n_{23}\Phi_{23}, n_{31}\Phi_{31}, n_{12}\Phi_{12})$ and $\vec{\mathcal{E}} = (n_{14}\Phi_{14}, n_{24}\Phi_{24}, n_{34}\Phi_{34})$.

We start from the effective EDM and MDM coupling in the nucleon-current vertex. The Dirac operator for the nucleon on a lattice is $\not{D} + m = \gamma^\mu(\partial_\mu + iQ\mathcal{A}_\mu) + m$, which we extend to include the pointlike effective interactions from Eq. (30):

$$\left[i\not{p} + m + iQ\mathcal{A}_q - \left(\frac{1}{2}\sigma^{\mu\nu}\mathcal{F}_{\mu\nu}\right)\frac{\kappa + i\zeta\gamma_5}{2m}\right]_{\mathcal{E}uc}, \tag{43}$$

with $\kappa = F_2(0)$ and $\zeta = F_3(0)$. We use the Euclidean matrices γ^μ (A4) and $[\gamma_5]_{\mathcal{E}uc} = (\gamma^1\gamma^2\gamma^3\gamma^4)_{\mathcal{E}uc}$ (A5)[3] and the plain-wave fields $\psi_p(x)$ and $\mathcal{A}_{q,\mu}(x)$ depending on the Euclidean four-momenta p, q as

$$\begin{aligned} &\psi_p(x) \propto e^{ipx}, \partial_\mu \psi_p(x) \leftrightarrow ip_\mu u_p; \\ &\mathcal{A}_{q,\mu}(x) \propto e^{i(p'-p)x} = e^{iqx}, \partial_\nu \mathcal{A}_{q,\mu}(x) \leftrightarrow iq_\nu \mathcal{A}_\mu. \end{aligned} \tag{44}$$

The mass m in the above equation (43) is chosen real and positive, since the chiral phase factor may be removed with a field redefinition (39), which at the same time rotates the dipole couplings (κ, ζ) into the physical magnetic and electric dipole moments, as has been shown in Sec. II B. After setting the charge $Q = 0$ and the momentum $\vec{p} = 0$, we use

$$\sigma^{ij}_{\mathcal{E}uc} = \epsilon^{ijk}\begin{pmatrix} -\sigma^k & \\ & -\sigma^k \end{pmatrix}, \quad \sigma^{i4}_{\mathcal{E}uc} = \begin{pmatrix} \sigma^i & \\ & -\sigma^i \end{pmatrix} \tag{45}$$

[3]The results are manifestly independent from the basis of γ-matrices used if the relation between γ_5 and γ^μ is kept unchanged.

and transform the operator (43) into the block-diagonal form, and find the condition for on-shell fermion energies

$$\begin{aligned} &\det\begin{pmatrix} \mathcal{M}_- & -E_0 \\ -E_0 & \mathcal{M}_+ \end{pmatrix} = 0 \Leftrightarrow \\ &\det(E_0^2 - \mathcal{M}_+\mathcal{M}_-) = \det(E_0^2 - \mathcal{M}_-\mathcal{M}_+) = 0, \end{aligned} \tag{46}$$

where

$$\mathcal{M}_\pm = m + \frac{1}{2m}(\kappa \mp i\zeta)(\vec{\mathcal{H}} \pm \vec{\mathcal{E}}) \cdot \vec{\sigma}. \tag{47}$$

The on-shell energies are then determined by the eigenvalues of the spin-dependent operator

$$\mathcal{M}_\mp \mathcal{M}_\pm = m^2 + \kappa\vec{\sigma}\cdot\vec{\mathcal{H}} - \zeta\vec{\sigma}\cdot i\vec{\mathcal{E}} + O(k^2, \zeta^2), \tag{48}$$

$$E_0 - m = \frac{\kappa}{2m}\vec{\mathcal{H}}\cdot\hat{\Sigma} - \frac{\zeta}{2m}i\vec{\mathcal{E}}\cdot\hat{\Sigma} + O(k^2, \zeta^2), \tag{49}$$

where $\hat{\Sigma}$ is the direction of the particle's spin. Note that the electric field enters Eq. (49) as $i\vec{\mathcal{E}}$, with an imaginary factor emphasizing that its value has been analytically continued to the imaginary axis, and the corresponding energy shift is purely imaginary. Equation (49) provides a prescription for extracting the EDM and MDM from mass shifts of a neutral particle on a lattice in uniform background fields.

III. cEDM-INDUCED EDM AND EDFF ON A LATTICE

In our initial calculation of cEDM-induced nucleon EDMs, we use two lattice ensembles with Iwasaki gauge action and $N_f = 2 + 1$ dynamical domain wall fermions: $16^3 \times 32$ with $m_\pi \approx 420$ MeV [25], and $24^3 \times 64$ with $m_\pi \approx 340$ MeV [26,27]. The ensemble parameters are summarized in Table I. We use identical ensembles, statistics, and spatial sampling per gauge configuration in both calculation methods discussed in further sections.

We use the *all-mode-averaging* framework [28] to optimize sampling, in which we approximate quark propagators with truncated CG solutions to a Möbius operator [29]. We use the Möbius operator with a short fifth dimension L_{5s} and complex s-dependent coefficients $b_s + c_s = \omega_s^{-1}$ (later referred to as "zMobius"), which approximates the same four-dimensional effective operator as the Shamir operator with the full $L_{5f} = 16$. The approximation is based on the equivelence between the domain wall and the overlap operators

$$\begin{aligned} [\not{D}^{\mathrm{DWF}}]_{4d} &= \frac{1 + m_q}{2} - \frac{1 - m_q}{2}\gamma_5 \epsilon_{L_5}(H_T), \\ H_T &= \gamma_5 \frac{\not{D}_W}{2 + \not{D}_W}, \end{aligned} \tag{50}$$

TABLE I. Lattice ensembles on which the simulations were performed. Both ensembles use Iwasaki gauge action and $N_f = 2+1$ domain wall fermions. The statistics are shown for "sloppy" (low-precision) samples. The nucleon masses were extracted using two-state fits. For the background electric field method, we quote the quantum of the electric field $\mathcal{E}_0 = \frac{6\pi}{a^2 L_t L_x}$.

$L_x^3 \times L_t \times L_5$	a [fm]	am_l	am_s	m_π [MeV]	m_N [GeV]	$\mathcal{E}_0$ [GeV^2]	Conf.	Stat.	N_{ev}	$N_{ev}^{\mathcal{E}=1,2}$	N_{CG}
$16^3 \times 32 \times 16$	0.114(2)	0.01	0.032	422(7)	1.250(28)	0.110	500	16000	200	150	100
$24^3 \times 64 \times 16$	0.1105(6)	0.005	0.04	340(2)	1.178(10)	0.0388	100	3200	200	200	200

$$\epsilon_{L_{5s}}^{\text{Möbius}}(x) = \frac{\prod_s^{L_{5s}}(1+\omega_s^{-1}x) - \prod_s^{L_{5s}}(1-\omega_s^{-1}x)}{\prod_s^{L_{5s}}(1+\omega_s^{-1}x) + \prod_s^{L_{5s}}(1-\omega_s^{-1}x)} \approx \epsilon_{L_{5f}}^{\text{Shamir}}(x), \tag{51}$$

where the coefficients ω_s are chosen so that the "sign" function $\epsilon_{L_{5s}}^{\text{Möbius}}(x)$ is the *minmax* approximation to the $\epsilon_{L_{5f}}^{\text{Shamir}}(x)$. We find that $L_{5s} = 10$ is enough for an efficient four-dimensional operator approximation. A shortened fifth dimension reduces the CPU and memory requirements: for example, $L_{5f} = 16$ is reduced to $L_{5s} = 10$, saving 38% of the cost. We deflate the low-lying eigenmodes of the internal even-odd preconditioned operator to make the truncated-CG AMA more efficient. The numbers of deflation eigenvectors N_{ev} and truncated CG iterations N_{CG} are given in Table I. We compute 32 sloppy samples per configuration. To correct any potential bias due to the approximation of the $\not{D}$ operator and the truncated CG inversion, in addition we compute one exact sample per configuration using the Shamir operator. The latter is computed iteratively by refining solutions of the "zMobius," again taking advantage of the short L_{5s} and deflation.

A. Parity-even and -odd nucleon correlators

The EDFF F_3 is a parity-odd quantity induced by $\not{C}\not{P}$ interactions. To compute the effect of CP-odd interactions, we modify the lattice action

$$S \to S + i\delta^{\overline{CP}} S = S + i\sum_{i,x} c_i [\mathcal{O}_i^{\overline{CP}}]_x, \tag{52}$$

where c_i are the CP-odd couplings such as the QCD θ angle, quark (chromo-)EDMs, etc. We Taylor-expand QCD + $\not{C}\not{P}$ vacuum averages in the couplings c_i. For example, for the three-point function, we get[4]

$$\begin{aligned}\langle N[\bar{q}\gamma^\mu q]\bar{N}\rangle_{\not{C}\not{P}} &= \frac{1}{Z}\int \mathcal{D}U\mathcal{D}\bar{\psi}\mathcal{D}\psi e^{-S-i\delta^{\overline{CP}}S} N[\bar{q}\gamma^\mu q]\bar{N} \\ &= C_{NJ\bar{N}} - i\sum_i c_i \delta_i^{\overline{CP}} C_{NJ\bar{N}} + O(c_\psi^2),\end{aligned} \tag{53}$$

[4]In this section, all conventions for correlators, form factors, and momenta are Euclidean.

where $C_{\dots}$ and $\delta^{\overline{CP}} C_{\dots}$ stand for CP-even and CP-odd correlators. Similarly, we also analyze the effect of $\not{C}\not{P}$ interaction on the nucleon-only correlators. In total, we calculate the following two- and three-point CP-even correlators as well as three- and four-point CP-odd correlators:

$$\begin{aligned}&C_{N\bar{N}} = \langle N\bar{N}\rangle, \quad \delta_i^{\overline{CP}} C_{N\bar{N}} = \langle N\bar{N}\sum_x [\mathcal{O}_i^{\overline{CP}}]_x\rangle, \\ &C_{NJ\bar{N}} = \langle N[\bar{q}\gamma^\mu q]\bar{N}\rangle, \quad \delta_i^{\overline{CP}} C_{NJ\bar{N}} = \langle N[\bar{q}\gamma^\mu q]\bar{N}\sum_x [\mathcal{O}_i^{\overline{CP}}]_x\rangle,\end{aligned}$$

where $\langle\cdots\rangle$ stand for vacuum averages computed with CP-even QCD action S. In Sec. III C, we also modify the action S to include a uniform background electric field as a probe of the electric dipole moment. In this work, we study only the quark chromo-EDM as the source of CP violation,

$$\mathcal{O}_{\psi G}^{\overline{CP}} = \frac{1}{2}\bar{\psi}[G_{\mu\nu}]^{\text{clov}}\sigma^{\mu\nu}\gamma_5\psi = \frac{1}{2}\bar{\psi}(g_S G_{\mu\nu}^{a,\text{cont}} T^a)\sigma^{\mu\nu}\gamma_5\psi, \tag{54}$$

where $G^{a,\text{cont}}$ is the continuum color field strength tensor and $[G_{\mu\nu}]^{\text{clov}}$ is the "clover" gauge field strength tensor on a lattice (see Fig. 3)

$$\begin{aligned}[G_{\mu\nu}]^{\text{clov}} = \frac{1}{8i}[&(U^P_{x,+\hat{\mu},+\hat{\nu}} + U^P_{x,+\hat{\nu},-\hat{\mu}} + U^P_{x,-\hat{\mu},-\hat{\nu}} + U^P_{x,-\hat{\nu},+\hat{\mu}}) \\ &- \text{H.c.}].\end{aligned} \tag{55}$$

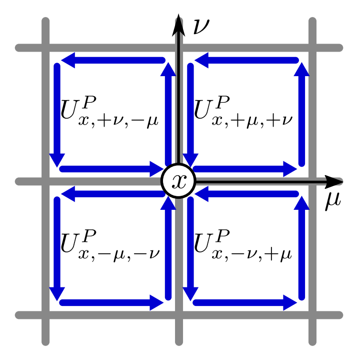

FIG. 3. "Clover" definition of the gauge field strength tensor on a lattice. The arrows correspond to products of gauge links taken around the plaquettes beginning and ending at point x.

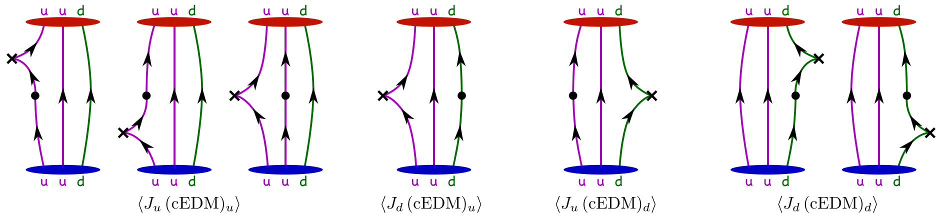

FIG. 4. Quark-connected contractions of the nucleon, quark current (dots), and cEDM operators (crosses).

Insertions of the quark-bilinear cEDM density (54) can generate both connected and disconnected contractions, similarly to the quark current. In this work, we calculate only the fully connected contributions to these correlation functions shown in Fig. 4. The disconnected contributions (see Fig. 5) are typically much more challenging to calculate, and we will address them in future work. Neglecting the disconnected diagrams will not affect the comparison of the form-factor and the energy-shift methods, because they are omitted in both calculations.

To compute the connected diagrams, we insert the quark-bilinear cEDM density (54) once in every ψ-quark line of $C_{NJ\bar{N}}$ diagrams, generating the four-point functions shown in Fig. 4. We evaluate all the connected three- and four-point contractions using the forward propagator and the set of sequential propagators shown in Fig. 6. In addition to the usual forward $\mathcal{F}$ and backward (sink-sequential) $\mathcal{B}$ propagators, we compute cEDM sequential $\mathcal{C}$ and doubly sequential ({cEDM, sink}-sequential) $(\mathcal{E}+\mathcal{G})$ propagators. For every additional value of the source-sink separation t_{sep} and the sink momentum $\vec{p}'$, additional backward $\mathcal{B}$ and doubly sequential $(\mathcal{E}+\mathcal{G})$ propagators must be computed, i.e.

$$N_{\mathcal{F}} = N_{\mathcal{C}} = 1, \qquad N_{\mathcal{B}} = N_q N_{\mathrm{sep}} N_{\mathrm{mom}},$$
$$N_{\mathcal{E}+\mathcal{G}} = N_q N_\psi N_{\mathrm{sep}} N_{\mathrm{mom}},$$

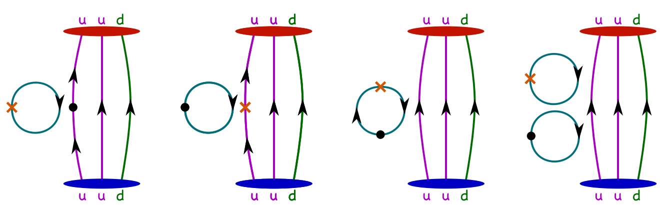

FIG. 5. Quark-disconnected contractions of the nucleon, quark current (dots), and cEDM operators (crosses).

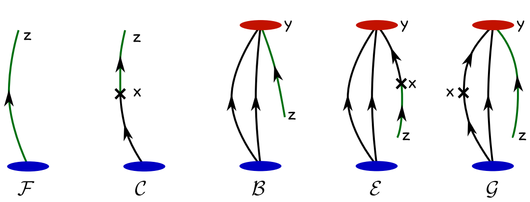

FIG. 6. Propagators required for computing quark-connected contractions of the nucleon, quark current, and cEDM operators.

where N_q is the number of separate flavors in the quark current and N_ψ is the number of separate flavors in the $\cancel{CP}$ operator. The connected CP-even two- and three-point correlators do not require any additional inversions. In this scheme, we perform only the minimal number of inversions required for computing all the diagrams for the neutron and proton EDMs induced by a *connected* flavor-dependent quark-bilinear $\cancel{CP}$ interaction with the two degenerate flavors u and d. Compared to Ref. [20], in which a small finite CP-odd perturbation term $\propto \epsilon$, $\epsilon \ll 1$ is added to the quark action resulting in modified quark propagators

$$\not{D}_m^{-1} \to (\not{D}_m + i\epsilon\sigma^{\mu\nu}\tilde{G}_{\mu\nu})^{-1}, \tag{56}$$

our four-point contractions correspond to computing the first derivative $(\partial C^\epsilon_{2,3}/\partial\epsilon)_{\epsilon=0}$ directly, thus avoiding any higher-order dependence on ϵ and obviating the ϵ-extrapolation. As a cross-check, we have verified our contraction code on a small test lattice by replacing propagators $\not{D}_m^{-1}\eta$ with

$$\not{D}_m^{-1}\eta \to [\not{D}_m^{-1} - \not{D}_m^{-1}(i\epsilon\Gamma)\not{D}_m^{-1}]\eta \tag{57}$$

to approximate $[\not{D}_m + i\epsilon\Gamma]^{-1}\eta$, where $\Gamma = \frac{1}{2}G_{\mu\nu}\sigma^{\mu\nu}\gamma_5$. Using these "$\overline{CP}$-perturbed" propagators, each of which required two inversions, we have computed the nucleon $C^\epsilon_{N\bar{N}}$ and the nucleon-current $C^\epsilon_{NJ\bar{N}}$ correlators, and compared their finite-difference ϵ-derivatives to $\delta C_{N\bar{N}}$ and $\delta C_{NJ\bar{N}}$.

We use only one value of the sink momentum $\vec{p}' = 0$. We compute nucleon-current three- and four-point correlators with two source-sink separation values $t_{\mathrm{sep}} = \{8, 10\}a = \{0.91, 1.15\}$ fm for the $16^3 \times 32$ ensemble, and three values $t_{\mathrm{sep}} = \{8, 10, 12\}a = \{0.88, 1.11, 1.33\}$ fm for the $24^3 \times 64$ ensemble. For the $24^3 \times 64$ lattice, we use the Gaussian-smeared sources with APE-smeared gauge links, using parameters optimized for overlap with the ground state [30], while for the $16^3 \times 32$ ensemble we use the smearing parameters from Ref. [11]. The effective nucleon mass plots from both ensembles are shown in Fig. 7. Correlators $C_{NJ\bar{N}}$ and $\delta^{\overline{CP}} C_{NJ\bar{N}}$ are computed with the polarization projector

$$T^+_{S_z+} = \frac{1+\gamma_4}{2}(1+\Sigma_z) = \frac{1}{2}(1+\gamma_4)(1-i\gamma_1\gamma_2), \tag{58}$$

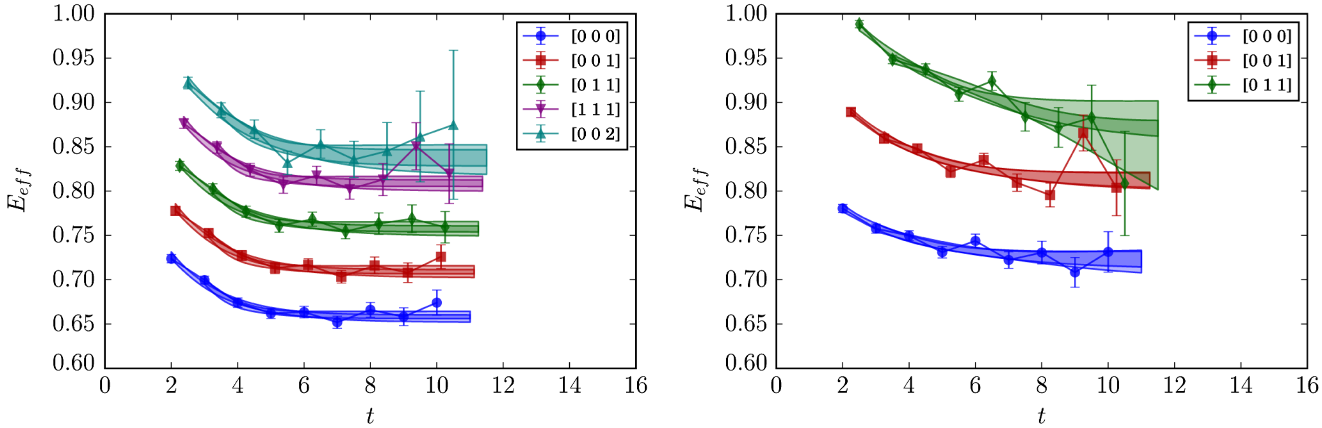

FIG. 7. Effective energy plots from the $24^3 \times 64$ (left) and $16^3 \times 32$ (right) lattices, together with two-state fits.

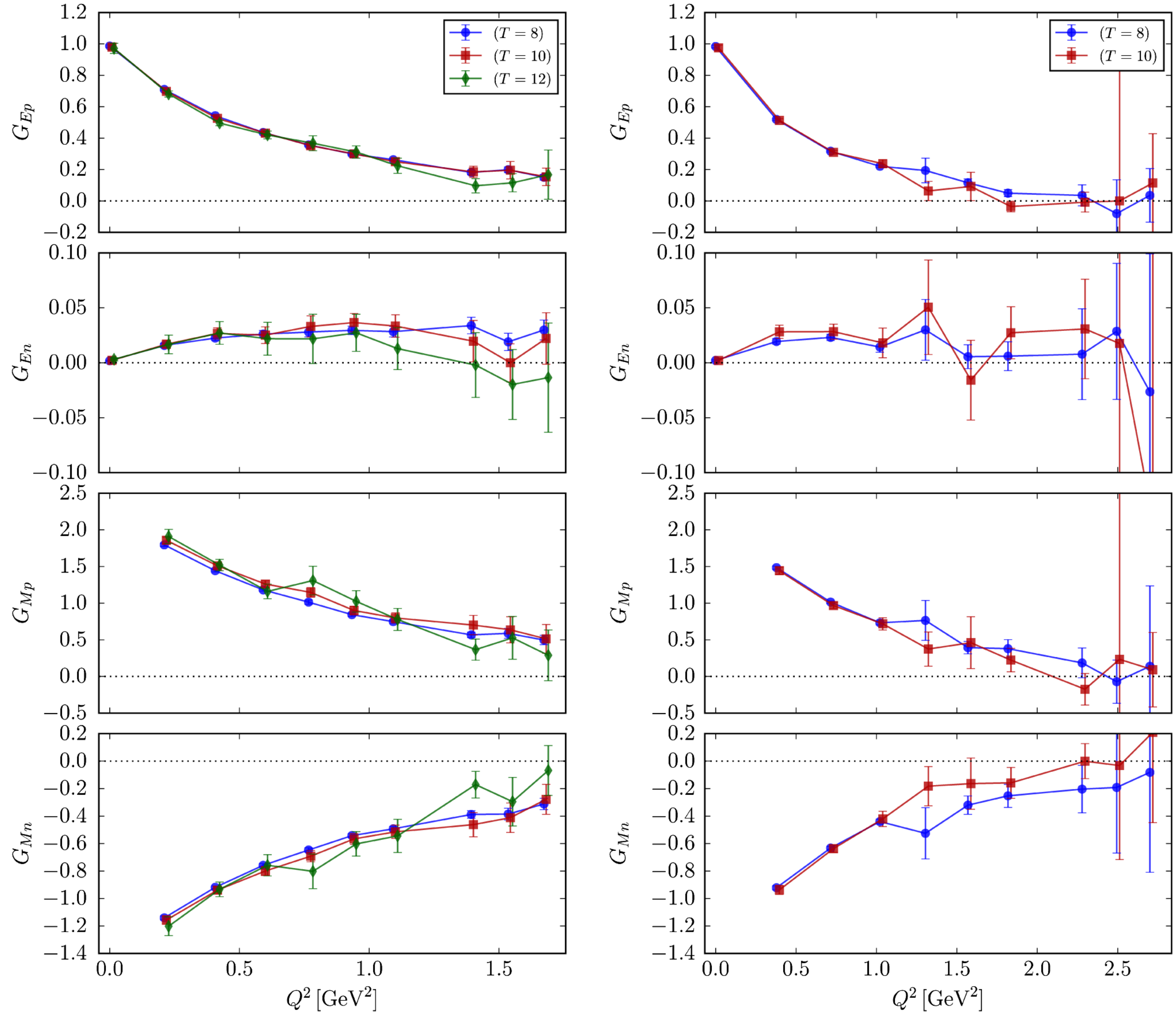

FIG. 8. Nucleon vector current form factors from the $24^3 \times 64$ (left) and $16^3 \times 32$ (right) lattices. Disconnected contractions are not included.

while correlators $C_{N\bar{N}}$ and $\delta^{\bar{C}P}C_{N\bar{N}}$ are computed with all 16 polarizations and saved to be used later for disconnected contractions. We reduce the cost of computing backward propagators with the widely used "coherent" trick, combining two backward sources from samples separated by $L_t/2$ into one inversion. Combining four samples resulted in a large increase in the statistical uncertainty, negating its cost-saving advantages.

B. Nucleon form factors

Following the discussion in Sec. II A, we use the form-factor decomposition that is different from those in the previous works [5–11]:

$$\langle N_{p'}|\bar{q}\gamma^\mu q|N_p\rangle = \bar{u}_{p'}\left[F_1(Q^2)\gamma^\mu + F_2(Q^2)\frac{\sigma^{\mu\nu}q_\nu}{2m_N} + F_3(Q^2)\frac{i\gamma_5\sigma^{\mu\nu}q_\nu}{2m_N}\right]u_p, \tag{59}$$

where the spinors u_p,$\bar{u}_{p'}$ have definite (positive) parity. Details of evaluating kinematic coefficients for form factors $F_{1,2,3}$ are given in Appendix C. We use the standard plateau method to evaluate both CP-even and CP-odd matrix elements of the nucleon,

$$[\delta^{\overline{CP}}]\mathcal{R}_{NJ\bar{N}}(t_{\mathrm{sep}},t_{\mathrm{op}}) = \frac{[\delta^{\bar{C}P}]C_{NJ\bar{N}}(t_{\mathrm{sep}},t_{\mathrm{op}})}{c_2'(t_{\mathrm{sep}})}\sqrt{\frac{c_2'(t_{\mathrm{sep}})}{c_2(t_{\mathrm{sep}})}\frac{c_2'(t_{\mathrm{op}})}{c_2(t_{\mathrm{op}})}\frac{c_2(t_{\mathrm{sep}}-t_{\mathrm{op}})}{c_2'(t_{\mathrm{sep}}-t_{\mathrm{op}})}}, \tag{60}$$

where the two-point functions are projected with the positive-parity polarization matrix $T^+ = \frac{1}{2}(1+\gamma_4)$,

$$c_2^{(\prime)}(t) = \mathrm{Tr}[T^+ C_{N\bar{N}}(\vec{p}^{(\prime)},t)]. \tag{61}$$

The averages of the three central points on the ratio plateaus are used as estimates of ground-state matrix elements. This is a crude estimate, and improved analysis of excited states is necessary for better control of systematic uncertainties. However, we find that our results change insignificantly when increasing the source-sink separation (see Figs. 9 and 13); therefore, we conclude that excited-state effects cannot influence the main conclusions of the paper.

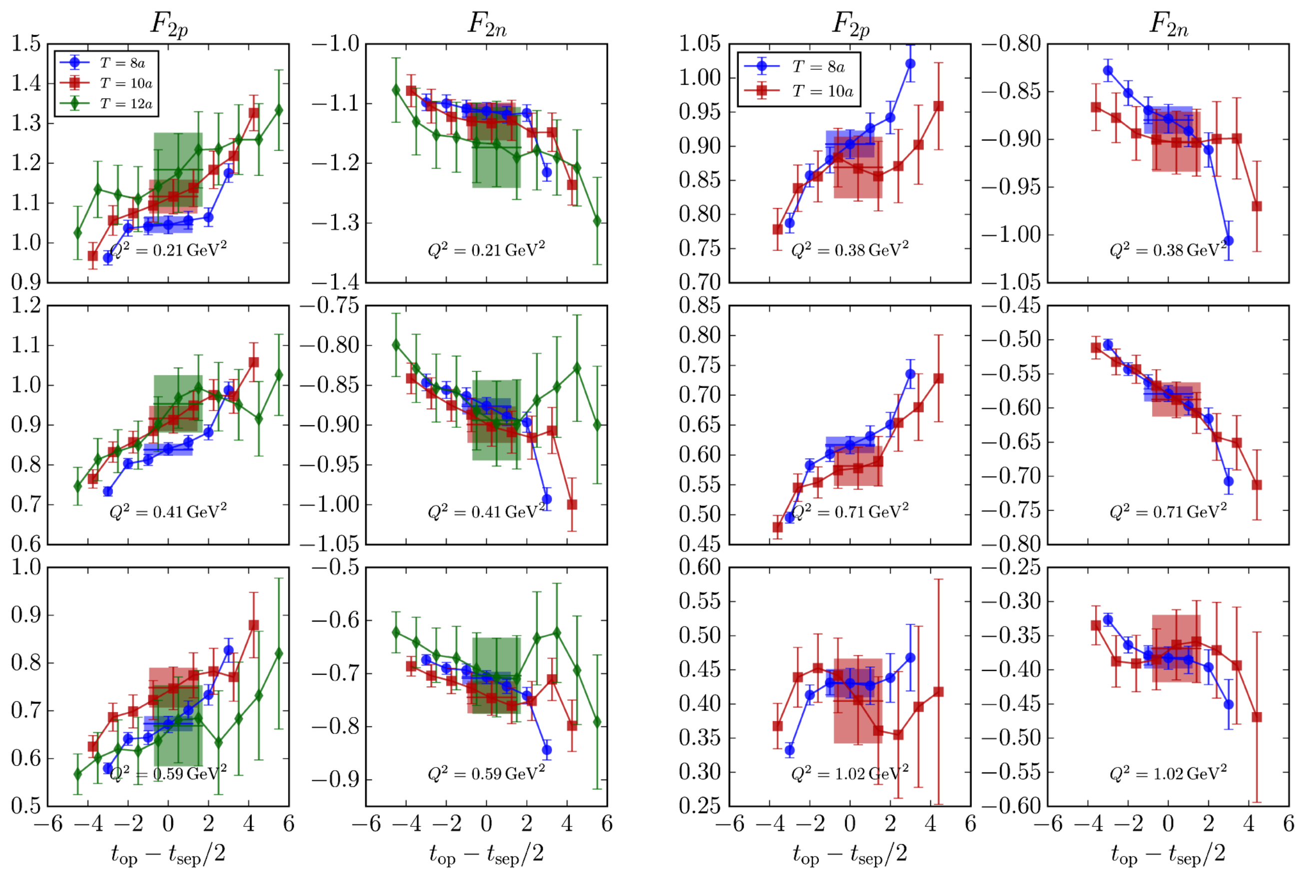

FIG. 9. Plateau plots for the neutron and proton Pauli form factors: the three smallest $Q^2>0$ points. Results are shown for the $24^3\times 64$ (left) and $16^3\times 32$ (right) lattices.

We calculate the Dirac and Pauli form factors $F_{1,2}$ using a correlated χ^2 fit to the matrix elements of the quark vector current ("overdetermined analysis"). The system of equations for form factors is reduced by combining equivalent equations to reduce the system dimension and make estimation of the inverse covariance matrix more stable (see, e.g., Ref. [30] for details). The quark-current operator is renormalized using renormalization constants $Z_V = 0.71408$ for $24^3 \times 64$ [27] and the chiral-limit value $Z_V = Z_A = 0.7162$ for $16^3 \times 32$ [31] ensembles. We show the momentum dependence of the resulting Sachs electric and magnetic form factors

$$\begin{aligned} G_E(Q^2) &= F_1(Q^2) - \frac{Q^2}{4m_N^2} F_2(Q^2), \\ G_M(Q^2) &= F_1(Q^2) + F_2(Q^2) \end{aligned} \tag{62}$$

for the proton and the neutron (connected only) for both ensembles in Fig. 8. Our data for form factors $G_{E,M}$ show no significant systematic variation with an increase of the source-sink separation $t_{\rm sep}$.

In order to compute the form factor F_3, we first need to calculate the parity mixing angle α_5 in order to subtract the $F_{1,2}$ mixing terms. Expanding the nucleon two-point function $C_{N\bar N}^{\not{C}\not{P}}(t)$ to the first order in $\alpha_5 \propto c_{\psi G}$ and assuming that the ground state dominates for a sufficiently large time t, we get

$$\begin{aligned} &C_{N\bar N}(t) - i c_{\psi G} \delta^{\overline{CP}} C_{N\bar N}(t) + O(c_{\psi G}^2) \\ &\overset{t\to\infty}{=} |Z_N|^2 \left[\frac{1+\gamma^4}{2} + i\alpha_5\gamma_5 + O(\alpha_5{}^2) \right] e^{-m_N t}. \end{aligned} \tag{63}$$

We use the projectors $T^+ = \frac{1+\gamma_4}{2}$ and $T^+\gamma_5$ to calculate the "effective" mixing angle $\hat\alpha_5(t)$ normalized to $c_{\psi G} = 1$,

$$\hat\alpha_5^{\rm eff}(t) = -\frac{{\rm Tr}[T^+\gamma_5 \delta^{\overline{CP}} C_{N\bar N}(t)]}{{\rm Tr}[T^+ C_{N\bar N}(t)]} \overset{t\to\infty}{=} \frac{\alpha_5}{c_{\psi G}}. \tag{64}$$

The time dependence of the ratios (64) for both ensembles is shown in Fig. 10. The quark flavors in the cEDM interaction are shown respective to the proton, and for the neutron $u \leftrightarrow d$ must be switched according to the isospin symmetry. The plateau is reached for time $t \geq 8$, and we extract the α_5 values from a constant fit (weighted average) to points $t = 8\ldots11$. An interesting observation is that the mixing angle depends very strongly on the flavor involved in the $\not{C}\not{P}$ interaction. Thus, for the proton $P_\delta = u_\delta(u^T C\gamma_5 d)$, in which the d quark is combined with the u quark into a scalar diquark, the d cEDM does not lead to any observable parity mixing.

Finally, the electric dipole form factor F_3 is calculated from the CP-odd four-point correlator $\delta^{\overline{CP}} C_{NJ\bar N}$. Similarly to the extraction of $\hat\alpha_5$ above, we expand the $\not{C}\not{P}$ three-point function in the CP-odd interaction. We extract the matrix elements using the ratios (60) of polarization-projected three-point functions ${\rm Tr}[T\mathcal{R}_{NJ\bar N}^{\not{C}\not{P}}]$ to CP-even two-point functions (61). Expanding the ratio in $\alpha_5 \propto c_{\psi G}$, we get

$$\begin{aligned} &{\rm Tr}[T(\mathcal{R}_{NJ\bar N} - i c_{\psi G}\delta^{\overline{CP}}\mathcal{R}_{NJ\bar N} + O(c_{\psi G}^2))] \\ &\overset{t\to\infty}{=} \sum_{i=1,2} [\mathcal{K}_{\mathcal{R}i}^{(T)} + i\alpha_5 \mathcal{K}_{\mathcal{R}i}^{(\{T,\gamma_5\})}] F_i + \mathcal{K}_{\mathcal{R}3}^{(T)} F_3 + O(\alpha_5{}^2), \end{aligned} \tag{65}$$

where $\mathcal{K}_{\mathcal{R}1,2,3}^{(T)}$ are the kinematic coefficients [Eqs. (C9)–(C12)] for form factors $F_{1,2,3}$ computed with the polarization matrix T and with $\mathcal{K} \to \mathcal{K}_\mathcal{R}$ (C14). Matching the $O(c_{\psi G})$ terms in the above expansion and neglecting excited states, we obtain

$$i\mathcal{K}_{\mathcal{R}3}^{(T)} \hat F_3 = {\rm Tr}[T\delta^{\overline{CP}}\mathcal{R}_{NJ\bar N}]_{g.s.} + \hat\alpha_5 \sum_{i=1,2} \mathcal{K}_{\mathcal{R}i}^{(\{T,\gamma_5\})} F_i. \tag{66}$$

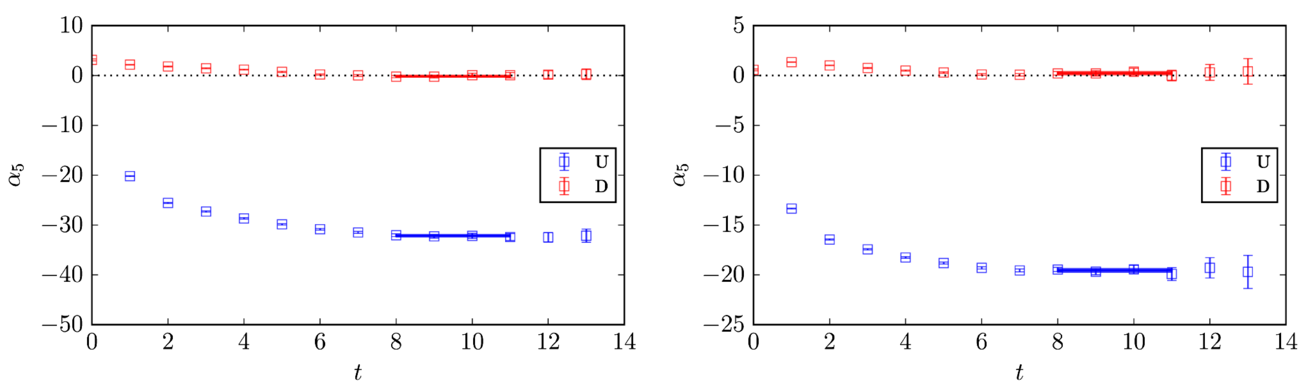

FIG. 10. Chiral rotation angle α_5 of the proton field induced by u- and d-quark cEDM interactions on the $24^3 \times 64$ (left) and $16^3 \times 32$ (right) lattices. The angles α_5 for the neutron are related by the $SU(2)_f$ symmetry $u \leftrightarrow d$. The chromo-EDM interactions are not renormalized and may contain mixing with other operators.

The second term on the rhs of the above equation is the mixing subtraction. Its form indicates that the mixing between form factors $F_{1,2}$ and F_3 happens only because of the polarization mixing of the nucleon interpolating fields on a lattice. This is substantially different from the expressions used in Refs. [5–11], which also include an additional subtraction term $(-2\alpha_5 F_3)$ because of the spurious mixing of F_2 and F_3 in the vector current vertex (24).

Although both timelike and spacelike components of the current can be used to calculate F_3, in practice we find that the time component J^4 yields much better precision than the spacelike component J^3. Due to the larger uncertainty of the J^3 signal, combining both components did not result in improved precision of the F_3 form factor. If only the J^4 component is used, the overdetermined fit to matrix elements is not required, and for $T = T^+_{S_z+} = \frac{1+\gamma_4}{2}(1 - i\gamma_1\gamma_2)$ from Eqs. (C10) and (C12),

$$(1+\tau)F_3(Q^2) = \frac{m_N}{q_3 \mathcal{K}_{\mathcal{R}}} \mathrm{Tr}[T^+_{S_z+} \delta^{\overline{CP}} \mathcal{R}_{N J^4 \bar{N}}] - \hat{\alpha}_5 G_E(Q^2), \tag{67}$$

where τ is the kinematic variable (C6). It is remarkable that for the neutron, the subtraction term $\propto \alpha_5 G_E$ is zero in the forward limit. In fact, if one uses the traditional formula for extracting the neutron EDM $d_N = F_3(0)/(2m_N)$, a large contribution $(-2\alpha_5 F_2(0))/(2m_N)$ comes from the spurious mixing if α_5 is not zero. In Sec. IV, we will discuss the

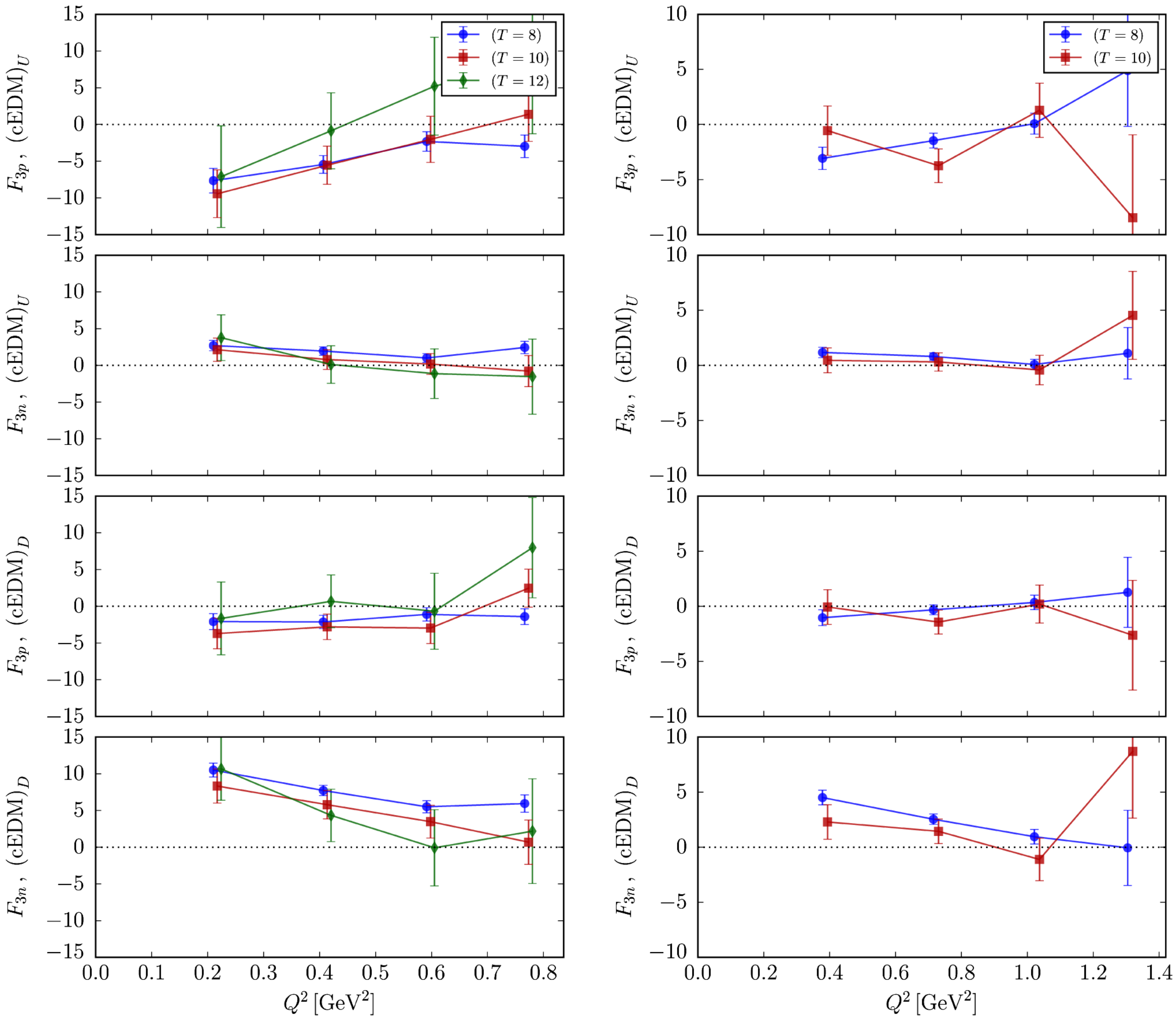

FIG. 11. Nucleon electric dipole form factors F_3 induced by u- and d-quark chromo-EDM interactions from the $24^3 \times 64$ (left) and $16^3 \times 32$ (right) lattices. The chromo-EDM interactions are not renormalized and may include mixing with other operators. Disconnected contractions are not included for either current or cEDM insertion.

currently available lattice results for the neutron and proton EDMs induced by the QCD θ term.

To compute form factors from data with each source-sink separation $t_{\rm sep}$, we use the value $\hat{\alpha}_5 = \hat{\alpha}_5^{\rm eff}(t_{\rm sep})$ in Eq. (67) to subtract the mixing. The results for the EDFF F_3 are shown in Fig. 11. Despite relatively high statistics, the signal for the cEDM-induced form factor is noisy. There is no significant dependence on the source-sink separation $t_{\rm sep}$. Since the cEDM operator is not renormalized, it can include contributions from other operators of dimension 5, as well as operators from lower dimension 3 [32]. One peculiar feature of these results is that, similarly to α_5, the contribution to the proton EDM comes mostly from the u cEDM, while the contribution to the neutron comes mostly from the d cEDM. However, a substantial increase in statistics, as well as a more elaborate analysis of excited states, is required to confirm these observations.

The electric dipole moment is determined by the value of the form factor $F_3(Q^2)$ at zero. This value is not directly calculable, and one has to extrapolate the $Q^2 > 0$ data points to $Q^2 = 0$. In Fig. 12, we show linear extrapolation of these form factors using the three smallest $Q^2 > 0$ points. Other fit models are not warranted until the statistical precision is substantially improved. We also show the comparison of three-point function plateaus in Fig. 13 with different source-sink separations.

C. Neutron electric dipole moments from energy shifts

Calculation of the dipole moment using a uniform background field has an advantage, in that no momentum extrapolation of form factors is required, because energy shifts depend on forward matrix elements of the nucleon. This calculation is easier for the neutron than for the proton: in the case of a charged particle, the analysis of its correlation function is more complicated due to its constant acceleration [22]. On the other hand, since the uniform background field is quantized on a lattice, these fields cannot be made arbitrarily small. In fact, the field quanta are very large, and their magnitudes are comparable to the QCD scale, especially on the smaller $16^3 \times 32$ lattice. Because of the fractional charges of quarks, the minimal value of the electric field contains an additional factor of 3, and it is quantized in multiples of $\mathcal{E}_0 = \frac{6\pi}{a^2 L_x L_t}$. The $\mathcal{E}_0$ values are shown in Table I, and for the smaller $16^3 \times 32$ lattice, the minimal electric field is $\mathcal{E}_0 = 0.110\ \mathrm{GeV}^2 = 560\ \mathrm{MV/fm}$. Such an electric field pulls the u quark in the neutron with tension $\approx(270\ \mathrm{MeV})^2$, or approximately 40% of the QCD string tension, and may deform the neutron too far away from the ground state.

We introduce the uniform electric field on a lattice as described in Sec. II C along the z direction. Using modified QCD + $U(1)$ gauge links, we calculate the regular nucleon correlator $C_{N\bar{N},\mathcal{E}}$, as well as the correlator with the insertion of CP-odd interaction, in full analogy with Sec. III A, e.g.,

$$\delta^{\overline{CP}} C_{N\bar{N},\mathcal{E}}(\vec{p},t) = \sum_{\vec{y}} e^{-i\vec{p}(\vec{y}-\vec{x})} \langle N(\vec{y},t)\bar{N}(\vec{x},0)\mathcal{O}_{\psi G}^{\overline{CP}}\rangle_{\mathcal{E}}. \tag{68}$$

The modified gauge links are used both in computing the propagators and in the construction of smeared sources and sinks. In fact, since the individual quarks are charged, smearing their distributions with the original QCD gauge links breaks gauge covariance and makes the calculation dependent on the choice of the gauge of the electromagnetic potential. The QCD links used in Gaussian smearing

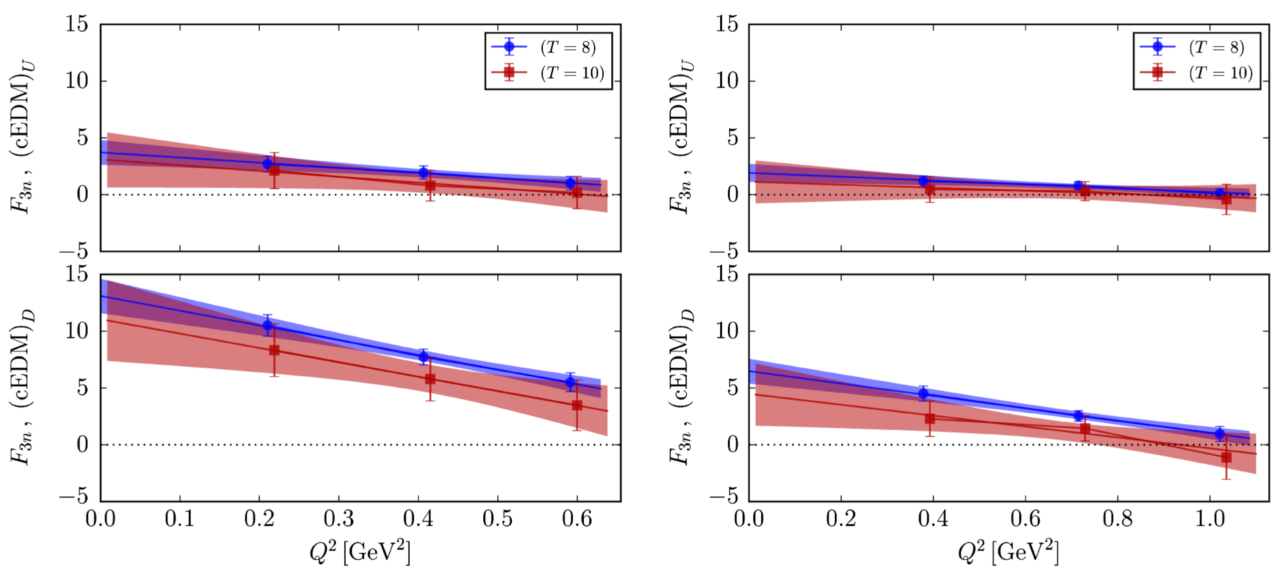

FIG. 12. Linear Q^2 fits to the neutron EDFF F_3 (same data as in Fig. 11) including only the three smallest $Q^2 > 0$ points and source-sink separations $T = 8a$, $10a$. Results are shown for the $24^3 \times 64$ (left) and $16^3 \times 32$ (right) lattices.

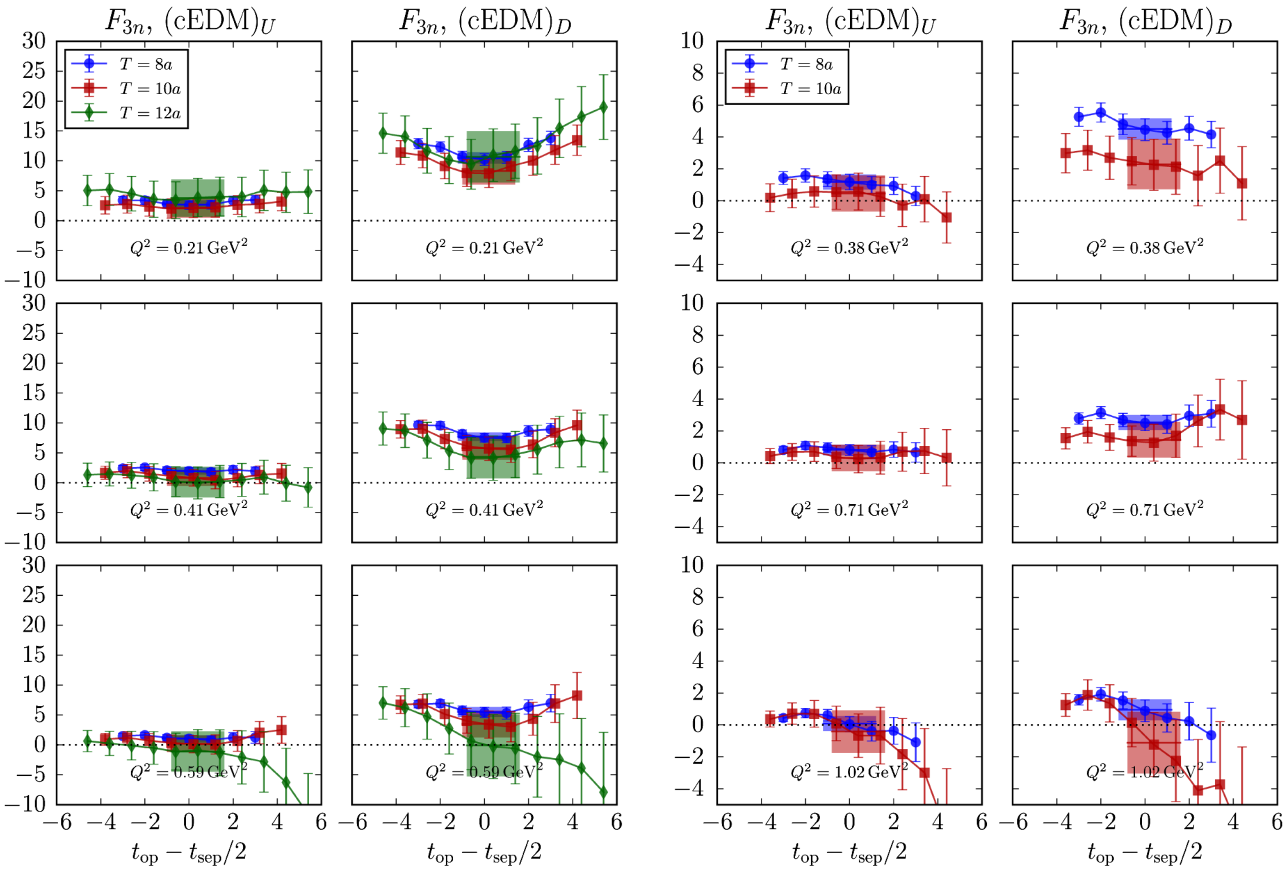

FIG. 13. Plateau plots for the neutron EDFF form factors: the three lowest $Q^2 > 0$ points. Results are shown for the $24^3 \times 64$ (left) and $16^3 \times 32$ (right) lattices.

are first APE-smeared, and then the electromagnetic potential is applied to them.

From Eq. (49), the energy of a particle on a lattice with the spin polarized along the electric field $\vec{\mathcal{E}} = \mathcal{E}\hat{z}$ is shifted by the imaginary value $\delta E = -(\zeta/2m)i\mathcal{E}$. The nucleon correlator at rest ($\vec{p} = 0$) thus must take the form

$$C^{\not{CP}}_{N\bar{N},\mathcal{E}}(\vec{p}=0,t) = |Z_N|^2 e^{i\alpha_5\gamma_5}\frac{1+\gamma_4}{2} \times \left[\frac{1+\Sigma_z}{2}e^{-(m+\delta E)t} + \frac{1-\Sigma_z}{2}e^{-(m-\delta E)t}\right]e^{i\alpha_5\gamma_5}. \tag{69}$$

As with the CP-odd form factor F_3, expanding the correlator up to the first order in α_5, δE, $\zeta \propto c_{\psi G}$, we get

$$C_{N\bar{N},\mathcal{E}} - ic_{\psi G}\delta^{\bar{CP}}C_{N\bar{N},\mathcal{E}} \overset{t\to\infty}{=} |Z_N|^2 e^{-m_N t}\left[\frac{1+\gamma_4}{2} + i\alpha_5\gamma_5 - \Sigma_z\delta E t\right], \tag{70}$$

and for the electric dipole moment we obtain the following estimator from the effective energy shift:

$$\zeta^{\mathrm{eff}}(t) = 2m_N d_N^{\mathrm{eff}}(t) = -\frac{2m_N}{\mathcal{E}_z}[R_z(t+1) - R_z(t)],$$
$$R_z(t) = \frac{\mathrm{Tr}[T^+\Sigma_z\delta^{\bar{CP}}C_{N\bar{N},\mathcal{E}_z}(t)]}{\mathrm{Tr}[T^+C_{N\bar{N},\mathcal{E}_z}(t)]}. \tag{71}$$

We have computed the neutron correlation functions with two values of the electric field $\mathcal{E} = \mathcal{E}_0$ and $2\mathcal{E}_0$. The results for both ensembles are shown in Fig. 14. We choose $t = 6\ldots9$ as the common plateau to estimate the value of ζ on both ensembles and both flavors in the cEDM operator. In the case of d cEDM, we observe nonzero values of the energy shift. Also, the EDM values computed with $\mathcal{E} = \mathcal{E}_0$ and $2\mathcal{E}_0$ agree well with each other, indicating that the energy shift is linear in $\mathcal{E}$ and our EDM result does not depend on the polarizing effect of the electric field on the nucleon.

D. Numerical comparison of the form-factor and energy-shift methods

The normalization and the sign convention of the dimensionless EDM ζ in Sec. III C are identical to those of $F_3(0)$ in Sec. III B, and we plot them for comparison in Fig. 15. We observe satisfactory agreement between the

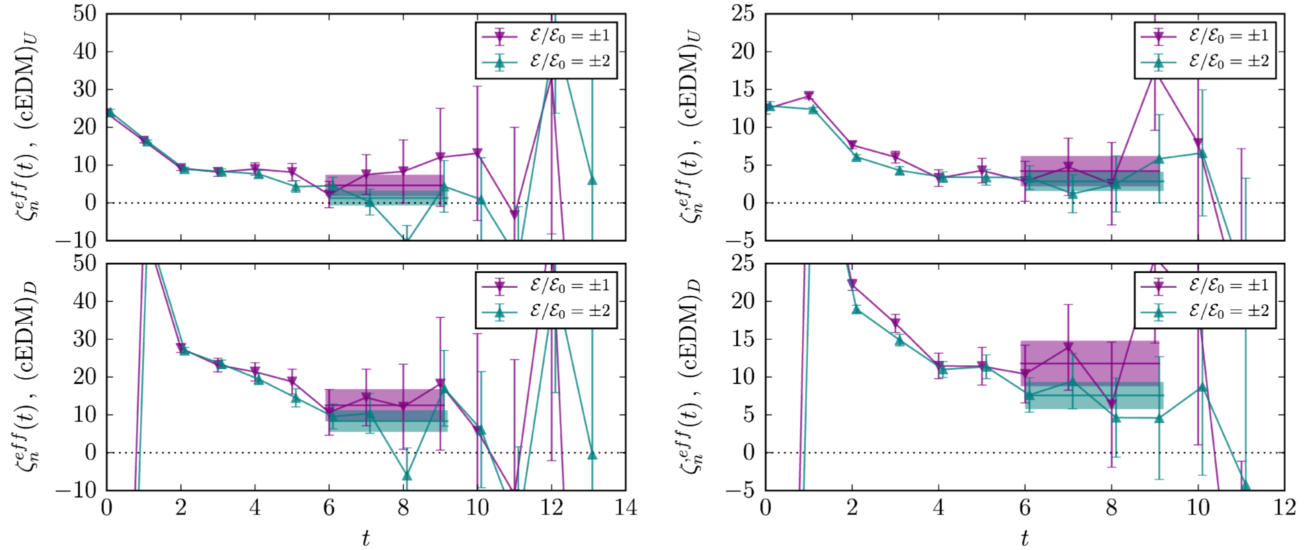

FIG. 14. The neutron EDM computed from energy shifts with two values of the electric field. The units are dimensionless, and the scale is the same as for F_3. The values used in comparison are computed as averages of the $t = 6\ldots9$ conservative plateaus common for both ensembles and both cEDM flavors. Results are shown for the $24^3 \times 64$ (left) and $16^3 \times 32$ (right) lattices.

values of ζ computed in the uniform background method and the values obtained from the $Q^2 \to 0$ extrapolation of form factors $F_{3n}(Q^2)$.

In order to check how the spurious mixing affects the results, in Fig. 15 we also plot the values of form factors computed with the old formula used in Refs. [5–11],

$$\tilde{F}_3 = F_3 - 2\alpha_5 F_2. \tag{72}$$

This formula obviously gives a value for $\tilde{F}_3$ different from F_3 only if α_5 is large. In the case of u cEDM, the value α_5 for the neutron is small, and there is no observable difference between F_3 and $\tilde{F}_3$. However, in the case of d cEDM, the difference is remarkable. None of the three sources of uncertainty—excited-state bias in the energy shift calculation, excited-state bias in the form-factor calculation, or the $Q^2 \to 0$ extrapolation of the form factors—can plausibly change the outcome of this comparison, due to the large value of α_5. The agreement between the new form-factor extraction formula and the energy-shift method is one of the main results of this paper, and serves as a numerical cross-check of our analytic derivation.

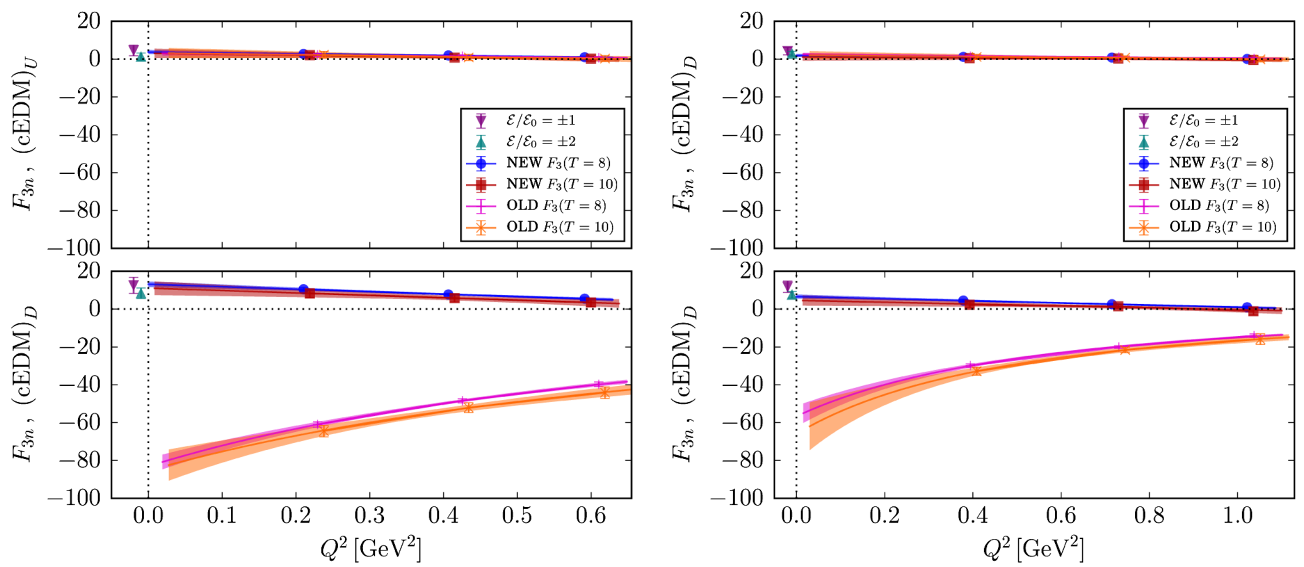

FIG. 15. Comparison of the neutron EDFF $F_{3n}(Q^2)$ computed with the conventional ("OLD") [5–11] and the "NEW" formula (C12) to the neutron EDM ζ computed from the energy shift (see Fig. 14). The "OLD" $F_{3n}(Q^3)$ data are extrapolated with the dipole fit, and the "NEW" with the linear fit. Data points are shifted horizontally for legibility. Results are shown for the $24^3 \times 64$ (left) and $16^3 \times 32$ (right) lattices.

TABLE II. Comparison of the neutron EDM ζ_n computed from the energy shift to the neutron forward EDFF $F_3(0)$ computed with the new formula (C12) and the old formula [5]. The parity mixing angle α_5 is computed from the plateaus in Fig. 10 (the flavors have been switched $u \leftrightarrow d$ to describe the neutron).

$24^3 \times 64$			
		$(\mathrm{cEDM})_U$	$(\mathrm{cEDM})_D$
α_5	$t = 8\ldots 11$	$-0.16(14)$	$-32.2(2)$
ζ_n from $\Delta E(\mathcal{E})$	$\mathcal{E}/\mathcal{E}_0 = 1$	4.6(2.8)	12.5(4.2)
	$\mathcal{E}/\mathcal{E}_0 = 2$	1.3(1.9)	8.4(2.8)
NEW $F_{3n}(0)$ [(C12)]	$T = 8a$	3.7(1.1)	13.1(1.5)
	$T = 10a$	3.1(2.4)	11.0(3.5)
OLD $F_{3n}(0)$ [5]	$T = 8a$	3.1(1.3)	$-80.8(3.8)$
	$T = 10a$	3.2(2.7)	$-82.4(8.2)$
$16^3 \times 32$			
α_5	$t = 8\ldots 11$	0.23(12)	$-19.54(15)$
ζ_n from $\Delta E(\mathcal{E})$	$\mathcal{E}/\mathcal{E}_0 = 1$	4.2(2.0)	11.8(3.0)
	$\mathcal{E}/\mathcal{E}_0 = 2$	2.8(1.3)	7.6(1.8)
NEW $F_3(0)$ [(C12)]	$T = 8a$	1.9(8)	6.5(1.1)
	$T = 10a$	1.1(1.9)	4.4(2.7)
OLD $F_3(0)$ [5]	$T = 8a$	2.5(9)	$-55.0(5.1)$
	$T = 10a$	2.1(2.1)	$-62.0(12.5)$

We collect the values of α_5, extrapolated $F_3(0)$, and ζ_n from the background field method in Table II.

IV. CORRECTIONS TO EXISTING θ-INDUCED nEDM LATTICE RESULTS

In Sec. II A, it has been shown that the commonly used formula for extracting the form factor F_3 from $\not{C}\not{P}$ nucleon matrix elements on a lattice is incorrect. This formula has been used in all of the papers that compute QCD θ-induced nucleon EDMs [5–11]. Fortunately, the correction has a very simple form (25), in which $\tilde{F}_{2,3}$ refer to the old results and $F_{2,3}$ refer to the corrected results. Unfortunately, Refs. [5–11] offer a broad spectrum of conventions for $\tilde{F}_3$ and α_5 differing in sign and scale factors. However, by comparing expressions for *polarized* CP-odd matrix elements of the timelike component of the vector current J_4, we can deduce the appropriate correction using that reference's conventions. For example, using Eq. (55) from Ref. [10],

$$\Pi^0_{3pt,Q}\left(\Gamma_k = \frac{i}{4}(1+\gamma_0)\gamma_5\gamma_k\right) \sim \frac{iQ_k}{2m_N}\left[\alpha^1\left(F_1 + \frac{E_N + 3m_N}{2m_N}F_2\right) + \frac{E_N + m_N}{2m_N}\tilde{F}_3\right] = \frac{iQ_k}{2m_N}[\alpha^1 G_E + (1+\tau)\underbrace{(\tilde{F}_3 + 2\alpha^1 F_2)}_{F_3}], \quad (73)$$

where $\tau = \frac{E_N - m_N}{2m_N}$ introduced in Eq. (C6), and $G_E = F_1 - \tau F_2$ is the Sachs electric form factor. Comparing the above equation to the expected form (C12), for the corrected value of F_3, we obtain

$$F_3(Q^2) = \tilde{F}_3(Q^2) + 2\alpha^1 F_2(Q^2), \quad (74)$$

which holds for any value of Q^2.

Although it is more suitable that the original authors of Refs. [5–11] reanalyze their data with these new formulas, it is interesting to examine whether the presently available lattice calculations yield nonzero values for the $\bar{\theta}$-induced nucleon EDMs after corrections similar to Eq. (74) have been applied. The most precise result for $F_{3n}(0)$ that also allows us to perform the correction unambiguously is Ref. [10], which reports an 8σ nonzero value for $F_3(0) = -0.56(7)$ from calculations with dynamical twisted-mass fermions at $m_\pi = 373$ MeV. However, when we apply the corresponding correction (74), the value becomes 0.09(7) and essentially compatible with zero.

Calculations with a finite imaginary θ angle [7,8] yield the most precise values of the neutron EDM to date. However, they do not contain sufficient details to deduce the proper correction for F_3. It must also be noted that it is not clear if the sign of the CP-odd interaction $\sim\tilde{G}G$ is consistent in all of the Refs. [5–11]. On the other hand, all the reported nonzero results for the proton and neutron EDM agree in sign so that $F_{3n}(0) < 0$ and $F_{3p}(0) > 0$, and it is *reasonable to assume* that any differences in the conventions are compensated in the final reported EDM values. Furthermore, because the θ angle is equivalent to a chiral rotation of quark fields, it is then *reasonable to assume* that upon conversion to some common set of conventions, e.g., those of Ref. [10], the sign of the chiral rotation angle α agrees between different calculations. Based on these plausible assumptions, we deduce that the results in Refs. [7,8] must be corrected as

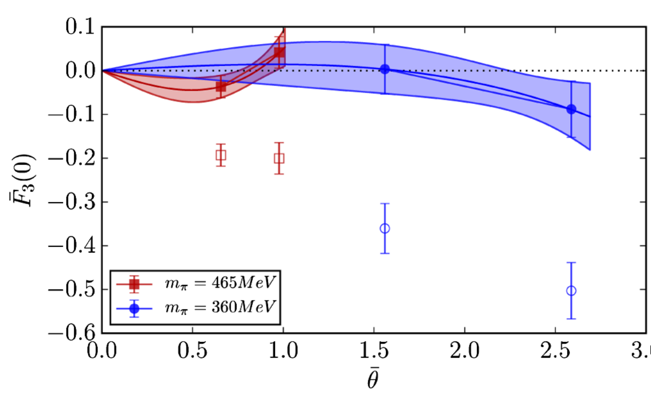

FIG. 16. Corrected (filled symbols) and original (open symbols) values for the neutron form factor F_3 at a nonzero imaginary θ angle from Ref. [8]. The linear parts in the limit $\theta \to 0$ are shown in Table III.

TABLE III. Corrections to the results reported in earlier calculations of $\bar{\theta}$-induced nucleon EDMs for the nucleon (n) and the proton (p). Some of the used values are at nonzero momentum transfer Q^2. Both form factors $F_{2,3}$ are quoted as dimensionless [in "magneton" units $e/(2m_N)$]. The errors for F_3 are taken equal to those of $\tilde{F}_3$ except for Ref. [8], in which the errors are extracted from our interpolation of the corrected $\bar{F}_3(\bar{\theta})$ values (see Fig. 16). In the first row, the correction follows the original conventions [10] exactly. In the following rows, the parity-mixing angles α have been transformed to $\alpha < 0$, and the EDMs have been corrected with $F_3 = \tilde{F}_3 + 2\alpha F_2$ using the assumptions discussed in the text.

		m_π [MeV]	m_N [GeV]	F_2	α	$\tilde{F}_3$	F_3
[10]	n	373	1.216(4)	−1.50(16)[a]	−0.217(18)	−0.555(74)	0.094(74)
[5]	n	530	1.334(8)	−0.560(40)	−0.247(17)[b]	−0.325(68)	−0.048(68)
	p	530	1.334(8)	0.399(37)	−0.247(17)[b]	0.284(81)	0.087(81)
[6]	n	690	1.575(9)	−1.715(46)	−0.070(20)	−1.39(1.52)	−1.15(1.52)
	n	605	1.470(9)	−1.698(68)	−0.160(20)	0.60(2.98)	1.14(2.98)
[8]	n	465	1.246(7)	−1.491(22)[c]	−0.079(27)[d]	−0.375(48)	−0.130(76)[d]
	n	360	1.138(13)	−1.473(37)[c]	−0.092(14)[d]	−0.248(29)	0.020(58)[d]

[a]Estimated as $(-\frac{1}{2}F_2^v(0))$ from Ref. [33], assuming $F_2^s \approx 0$.
[b]The value f_{1n} was reported incorrectly in Ref. [5] with a factor of $\frac{1}{2}$ [34].
[c]From Ref. [35], where F_2 was computed with $\bar{\theta} = 0$.
[d]Estimated from a linear + cubic fit to plotted $\bar{\alpha}(\bar{\theta})$ and F_3^θ data [8].

$F_3^\theta = \tilde{F}_3^\theta + 2\alpha(\theta)F_2$,[5] where $\alpha < 0$, in analogy with Ref. [10]. The data for $\bar{\alpha}^\theta$ and $\tilde{F}_3^\theta(0)$ at finite $\bar{\theta}$ values are extracted from figures in Ref. [8]. The original $\tilde{F}_3^\theta(0)$ and the corrected $F_3^\theta(0)$ values are shown in Fig. 16. Following Ref. [8], the corrected $F_3^\theta(0)$ values are interpolated to $\bar{\theta} \to 0$ using a linear + cubic fit $F_3(0)\bar{\theta} + C\bar{\theta}^3$, and the resulting values $F_3(0) = dF_3^\theta/d\bar{\theta}|_{\bar{\theta}=0}$ are given in Table III. We observe that the corrected values at both the finite and zero $\bar{\theta}$ values agree with zero at the $\lesssim 2\sigma$ level.

Corrections to other results [5,6] may be done on a similar basis.[6] The resulting values are also collected in Table III, and in all cases they are compatible with zero, deviating at most 2σ. We emphasize that, apart from Ref. [10], these corrections are made using the sign assumptions discussed above. If our assumptions are wrong, the corrected central values will be approximately twice as large compared to the originally reported values. Although we find our assumptions *plausible*, and thus the corrected values in Table III most likely valid, a final confirmation of our findings can only be done if the authors of Refs. [5–9,11] reanalyze their data with our correction. It is possible that the difference between the lattice values of the neutron EDM and phenomenological estimates $d_n \sim O(10^{-3}\ldots10^{-2})\bar{\theta}e$ fm [12,14,18,36], which has been ascribed to chiral symmetry breaking of lattice fermions and heavy quark masses used in the simulations, can disappear when the proper corrections are applied.

[5]Strictly speaking, for finite values of $\bar{\theta}$ and $\bar{\alpha}(\bar{\theta})$, one has to use the hyperbolic "rotation" formula $\cosh(2\alpha)F_3 = \tilde{F}_3 + \sinh(2\alpha)F_2$. We neglect $O(\alpha^2)$ terms because $|\alpha| \lesssim 0.15$, while the precision is only $\approx 10\%$.

[6]Correction to the result in Ref. [7] requires the corresponding values for F_2, which we could not locate in published works.

V. SUMMARY AND CONCLUSIONS

Among our most important findings in this paper are the new formula for the analysis of nucleon-current correlators computed in a $\not{C}\not{P}$ vacuum and the extraction of the electric dipole form factor F_3. We have demonstrated, both analytically and numerically, that the analyses of the $\bar{\theta}$-induced nucleon EDM in previous calculations [5–11] introduced spurious contributions $(-2\alpha_5\kappa)$ due to mixing with the anomalous magnetic moment κ of the nucleon. Fortunately, the correction is very simple and requires only the values of the nucleon anomalous magnetic moments from calculations on the same lattice ensembles. Applying this correction properly is somewhat complicated, due to differences in the conventions used in these works. Under some *plausible* assumptions we have demonstrated that, after the correction, even the most precise current lattice results for $\bar{\theta}$ nEDMs may be compatible with zero. If this finding is confirmed in detailed reanalyses of Refs. [5–11], the precision of the current lattice QCD determination of $\bar{\theta}$ nEDMs may be completely inadequate *to constrain* the QCD $\bar{\theta}$ angle from experimental data. The entire modern program to search for fundamental symmetry violations as signatures of new physics relies on our understanding of the effects of quark and gluon $\not{C}\not{P}$ interactions on nucleon structure. The importance and urgency of first-principles calculations of these effects hardly needs more emphasis, and we conclude that they will likely be even more difficult than thought before.

In this paper, we have also performed calculations of the nucleon electric dipole moments induced by CP-odd quark-gluon interactions using two different methods. In the first method, we have successfully calculated the nucleon-current correlators with and without the CP-odd interaction, evaluating up to four-point connected nucleon correlation functions. We have demonstrated that this novel technique works well, and we argue that it is both cheaper and has fewer uncertainties than the technique used in Refs. [20,21] to compute the same observables with modified Wilson action. One of the obstacles to applying the technique of Refs. [20,21] is that low-eigenmode deflation used to accelerate calculations will be more expensive, because new eigenvectors have to be computed for every modification of the fermion action. This may also be partially true for recently introduced multi-grid methods, in which null-subspace vectors of a Dirac operator have to be computed in a setup phase, which has considerable cost.

In the second method, we computed the neutron EDM using its energy shift in a uniform background electric field and in the presence of the same CP-odd interaction. The energy-shift method to compute nucleon EDM has been used before [2–4], but our calculation is the first one that uses the uniform background electric field respecting boundary conditions [22]. We perform calculations with identical statistics in both methods and can directly compare the central values and the uncertainties of the results. We find that the EDM results agree if the new formula for extraction of the EDFF F_3 is used. Also, both methods yield comparable uncertainty, and the energy-shift method may be preferable in the future because it does not require forward-limit extrapolation, and excited states may be easier to control [37].

Our calculations on a lattice are far from perfect and require improvement of the treatment of excited states and the forward-limit extrapolation of the form factors. However, the associated systematic uncertainties are too small to cast doubt on the numerical comparison of the energy shift and the form-factor methods. Although our calculations lack evaluation of the disconnected diagrams and renormalization and mixing subtractions of the quark chromo-EDM operator, these drawbacks apply equally to both methods, and therefore do not affect said validation.

Future calculation of disconnected contributions to the F_3 form factors will be an extension to the present work, in which the quark-disconnected loops with insertions of the quark current, chromo-EDM, and both, will be evaluated and used together with the existing nucleon correlators. The disconnected contractions do not require four-point correlators and are simpler to construct, although the stochastic noise will likely be a much bigger problem than for the connected contractions. We expect that with advances in numerical evaluation of the disconnected diagrams [38], this problem will be tractable.

ACKNOWLEDGMENTS

T. B. is supported by U.S. Department of Energy Grant No. DE-FG02-92ER40716. T. I. is supported in part by U.S. Department of Energy Contracts No. AC-02-98CH10886 and No. DE-SC0012704 (Brookhaven National Laboratory). S. A. and T. I. are also supported in part by the Grant-in-Aid of the Japanese Ministry of Education, Sciences and Technology, Sports and Culture (MEXT) for Scientific Research (No. JP16H03978, No. JP17H02906, and No. 26400261), by *a priority* issue (Elucidation of the Fundamental Laws and Evolution of the Universe) to be tackled by using the “Post-K” computer, and by the Joint Institute for Computational Fundamental Science (JICFuS). H. O. is supported by the RIKEN Special Postdoctoral Researcher program. S. N. S. is supported by the Nathan Isgur fellowship program at JLab and by RIKEN BNL Research Center under its joint tenure track fellowship with Stony Brook University. S. A. and S. N. S. are also grateful for the hospitality of the Kavli Institute for Theoretical Physics (UC Santa Barbara) during the “Nuclear16” workshop. This research was supported in part by the National Science Foundation under Grant No. NSF PHY11-25915. Gauge configurations with dynamical domain wall fermions used in this work were generated by the RBC/UKQCD Collaboration. The computation was performed using the Hokusai supercomputer of the RIKEN ACCC facility and the Jlab cluster as part of the USQCD Collaboration. The calculations were performed with the “Qlua” software suite [39]. This material is based upon work supported by the U.S. Department of Energy, Office of Science, Office of Nuclear Physics under Contract No. DE-AC05-06OR23177. Contributions to this article by workers at NIST, an agency of the U.S. Government, are not subject to U.S. copyright.

APPENDIX A: CONVENTIONS

In this appendix, we collect conventions for γ-matrices implicitly or explicitly used throughout the text. In Table IV, we also provide notes on the transformation between Minkowski ($\mathcal{M}2$) and Euclidean ($\mathcal{E}uc$) notations to avoid any ambiguities in matching Minkowski and

TABLE IV. Correspondence between notations used in Minkowski $\mathcal{M}2$ (metric $\{-,-,-,+\}$) and Euclidean $\mathcal{E}uc$ spacetime. Upon transition $\mathcal{M}2 \leftrightarrow \mathcal{E}uc$, the quantities in the corresponding columns transform into each other.

Quantity	$[*]_{\mathcal{M}2}$	$[*]_{\mathcal{E}uc}$
Coordinate	$(\vec{x}, t) = (x^i, x^4)$	$(x^i, -ix^4)$
Momentum	$(\vec{p}, E) = (p^i, p^4)$	$(p^i, -ip^4)$
Scalar product	$a^\mu b_\mu$	$(-a^\mu b_\mu)$
Plane wave	$e^{-ipx} = e^{-iEt+i\vec{p}\,\vec{x}}$	$e^{ipx} = e^{-Ex^4+i\vec{p}\,\vec{x}}$
γ-matrices	(γ^i, γ^4)	$(i\gamma^i, \gamma^4)$
“Slashed” vector	$\not{p} = p^\mu \gamma_\mu$	$(-i\not{p}) = (-ip^\mu \gamma_\mu)$
Dirac operator	$(\not{p} - m)$	$(i\not{p} + m)$
Spin matrix $\sigma^{\mu\nu}$	$(\sigma^{ij}, \sigma^{i4})$	$(-\sigma^{ij}, i\sigma^{i4})$
Spin matrix $\sigma^{\mu\nu} q_\nu$	$(\sigma^{i\nu} q_\nu, \sigma^{4\nu} q_\nu)$	$(\sigma^{i\nu} q_\nu, -i\sigma^{4\nu} q_\nu)$

Euclidean form-factor expressions for matrix elements and vertices.

In Minkowski space with metric $\{-1,-1,-1,+1\}$, we use the chiral γ-matrix basis

$$[\gamma^i]_{\mathcal{M}2} = \begin{pmatrix} & \sigma^i \\ -\sigma^i & \end{pmatrix}, \qquad [\gamma^4]_{\mathcal{M}2} = \begin{pmatrix} & 1 \\ 1 & \end{pmatrix}, \tag{A1}$$

and with $\epsilon^{4123} = +1$, we define the chiral γ_5 matrix

$$\begin{aligned}[\gamma_5]_{\mathcal{M}2} &= -\frac{i}{4!}[\epsilon^{\mu\nu\rho\sigma}\gamma_\mu\gamma_\nu\gamma_\rho\gamma_\sigma]_{\mathcal{M}2} = i[\gamma^4\gamma^1\gamma^2\gamma^3]_{\mathcal{M}2} \\ &= \begin{pmatrix} -1 & \\ & 1 \end{pmatrix}.\end{aligned} \tag{A2}$$

For the spin matrix $\sigma^{\mu\nu} = \frac{i}{2}[\gamma^\mu,\gamma^\nu]$, we will also need the relation

$$[\sigma^{\mu\nu}\gamma_5]_{\mathcal{M}2} = \frac{i}{2}[\epsilon^{\mu\nu\rho\sigma}\sigma_{\rho\sigma}]_{\mathcal{M}2}. \tag{A3}$$

In accordance with Table IV, the γ-matrices in Euclidean spacetime are

$$[\gamma^i]_{\mathcal{E}uc} = \begin{pmatrix} & -i\sigma^i \\ +i\sigma^i & \end{pmatrix}, \qquad [\gamma^4]_{\mathcal{E}uc} = \begin{pmatrix} & 1 \\ 1 & \end{pmatrix}, \tag{A4}$$

in which $\gamma^{1,3}$ have the opposite sign compared to the deGrand-Rossi basis used in most of the lattice QCD software. This difference is inconsequential, because all results are manifestly covariant with respect to unitary basis transformations. Finally, we use the γ_5 definition that agrees with the lattice software,

$$[\gamma_5]_{\mathcal{E}uc} = [\gamma^1\gamma^2\gamma^3\gamma^4]_{\mathcal{E}uc} = \begin{pmatrix} 1 & \\ & -1 \end{pmatrix}, \tag{A5}$$

and note that the kinematic coefficients for vector form factors derived in Appendix C depend on a particular γ_5 definition in terms of γ^μ, but the numerical lattice results are invariant as long as the same $[\gamma_5]_{\mathcal{E}uc}$ is used in both Eqs. (54) and (30).

APPENDIX B: ELECTRIC AND MAGNETIC DIPOLE MOMENTS AND FORM FACTORS

In this appendix, we recall the connection between the form factors $F_{2,3}$ and the magnetic and electric dipole moments of a spin-1/2 particle. Although this is discussed in many textbooks, we find it useful to perform a rigorous derivation expanding the matrix element (14) in the momentum transfer $q = p' - p$ and taking the limit $q \to 0$. For completeness and to avoid any ambiguities, in addition to the γ-matrices in Appendix A, we collect all relevant conventions for EM fields, 4-spinors, and their interaction. The discussion in this appendix assumes Minkowski conventions $\mathcal{M}2$ with $g_{\mu\nu} = \mathrm{diag}\{-1,-1,-1,+1\}$.

The charged fermion-photon interaction is determined by the form of the "long" derivative,

$$\begin{aligned}&D_\mu = \partial_\mu + ieA_\mu, \\ &\mathcal{L} = \bar\psi(iD_\mu\gamma^\mu - m)\psi = \bar\psi(i\partial\!\!\!/ - m)\psi - eA_\mu J^\mu,\end{aligned} \tag{B1}$$

which leads to the interaction Hamiltonian

$$\begin{aligned}H_{\rm int} &= \int d^3x(-\mathcal{L}_{\rm int}) = e\int d^3x A_\mu J^\mu \\ &= e\int d^3x(\rho\phi - \vec J\cdot\vec A),\end{aligned} \tag{B2}$$

where the EM potential $A^\mu = (\vec A,\phi)$, EM current $J^\mu = (\vec J,\rho)$, and the electric coupling (charge) $e = |e|$.

To evaluate the matrix element (14) in the interaction (B2), we use the chiral γ-matrix representation summarized in Appendix A. The on-shell spinors satisfying the regular Dirac equation with a real-valued mass $m > 0$ and energy $E^{(\prime)} = \sqrt{m^2 + \vec p^{(\prime)2}}$ take the form

$$\begin{aligned}u_p &= \begin{pmatrix}\sqrt{E - \vec p\vec\sigma}\xi \\ \sqrt{E + \vec p\vec\sigma}\xi\end{pmatrix} = \sqrt{m}\left[1 + \frac{\vec p\vec\Sigma}{2m}\gamma_5 + O(\vec p^2)\right]\begin{pmatrix}\xi \\ \xi\end{pmatrix}, \\ \bar u_{p'} &= \begin{pmatrix}\sqrt{E' - \vec p'\vec\sigma}\xi' \\ \sqrt{E' + \vec p'\vec\sigma}\xi'\end{pmatrix}^\dagger\gamma^4 = \sqrt{m}\begin{pmatrix}\xi' \\ \xi'\end{pmatrix}^\dagger\left[1 - \frac{\vec p'\vec\Sigma}{2m}\gamma_5 + O(\vec p^2)\right],\end{aligned} \tag{B3}$$

where

$$\Sigma^k = \frac{1}{2}\epsilon^{ijk}\sigma^{jk} = \begin{pmatrix}\sigma^k & \\ & \sigma^k\end{pmatrix}.$$

We will use these spinors to evaluate matrix elements of the Hamiltonian (B2), treating the EM field as classical background. Note that in order to treat these matrix elements as the interaction energy, the states must be normalized as nonrelativistic:

$$\begin{aligned}E_{\rm int} &= \langle\vec p',\sigma'|H_{\rm int}|\vec p,\sigma\rangle_{\rm NR} \\ &= eA_\mu\frac{1}{\sqrt{2E'2E}}\bar u_{p'}\Gamma^\mu(p',p)u_p \doteq eA_\mu\langle\langle\Gamma^\mu\rangle\rangle,\end{aligned} \tag{B4}$$

where we have introduced the notation $\langle\langle X\rangle\rangle = \frac{1}{\sqrt{2E'2E}}\bar u_{p'}Xu_p$ for convenience, and Γ^μ was introduced in Eq. (15). In the limit of small spatial momenta $|\vec p|$, $|\vec p'| \to 0$, only the spatial components σ^{ij} give nonvanishing contributions when contracted with the spinors (B3):

$$\langle\!\langle\sigma^{ij}\rangle\!\rangle = \frac{1}{\sqrt{2E2E'}}\bar{u}_{p'}\sigma^{ij}u_p = \epsilon^{ijk}\xi'^{\dagger}\sigma^k\xi + O(|\vec{p}|,|\vec{p}'|),$$
$$\langle\!\langle\sigma^{4k}\rangle\!\rangle = \bar{u}_{p'}\sigma^{4k}u_p = O(|\vec{p}|,|\vec{p}'|). \tag{B5}$$

Recalling the conventions [40] for the EM potential A^μ,

$$(\vec{E})^i = -\frac{\partial}{\partial x^i}A^4 - \frac{\partial}{\partial t}(\vec{A})^i, \tag{B6}$$

$$(\vec{H})^i = (\mathrm{curl}\vec{A})^i = \epsilon^{ijk}\frac{\partial}{\partial x^j}(\vec{A})^k, \tag{B7}$$

which result in the following field strength tensor $F_{\mu\nu}$ and its dual $\tilde{F}_{\mu\nu} = \frac{1}{2}\epsilon_{\mu\nu\rho\sigma}F^{\rho\sigma}$, $\epsilon_{1234} = +1$:

$$F_{\mu\nu} = \begin{array}{c@{}c} & \begin{array}{cccc} 1 & 2 & 3 & 4 \end{array} \\ \begin{array}{c} 1 \\ 2 \\ 3 \\ 4 \end{array} & \begin{pmatrix} 0 & -H^3 & H^2 & -E^1 \\ H^3 & 0 & -H^1 & -E^2 \\ -H^2 & H^1 & 0 & -E^3 \\ E^1 & E^2 & E^3 & 0 \end{pmatrix} \end{array}, \tag{B8}$$

$$\tilde{F}_{\mu\nu} = \begin{array}{c@{}c} & \begin{array}{cccc} 1 & 2 & 3 & 4 \end{array} \\ \begin{array}{c} 1 \\ 2 \\ 3 \\ 4 \end{array} & \begin{pmatrix} 0 & E^3 & -E^2 & -H^1 \\ -E^3 & 0 & E^1 & -H^2 \\ E^2 & -E^1 & 0 & -H^3 \\ H^1 & H^2 & H^3 & 0 \end{pmatrix} \end{array}, \tag{B9}$$

where the rows and the columns are enumerated by μ and ν, respectively. With the following conventions for the fermion and photon fields with definite momenta $p^{(\prime)}$ and q, respectively:

$$\psi_p(x) \sim e^{-ipx}, \qquad \bar{\psi}_{p'}(x) \sim e^{ip'x},$$
$$A_{q,\mu}(x) \sim e^{-i(p'-p)x} = e^{-iqx}, \tag{B10}$$

the derivatives acting on these fields are translated into factors of momenta,

$$\not{\partial}\psi = \gamma^\mu\partial_\mu\psi \to \gamma^\mu(-ip_\mu)\psi = (-i)\not{p}\psi, \tag{B11}$$

$$F_{\mu\nu}(x) = \partial_\mu A_\nu - \partial_\nu A_\mu \to (-i)(q_\mu A_\nu - q_\nu A_\mu). \tag{B12}$$

Applying the Gordon identity to Eq. (14) and omitting the F_A form factor, we get

$$\langle p',\sigma'|J^\mu|p,\sigma\rangle_{\not{C}\not{P}}$$
$$= \bar{u}_{p'}\left[F_1\frac{(p'+p)^\mu}{2m} + (G_M + i\gamma_5F_3)\frac{i\sigma^{\mu\nu}q_\nu}{2m}\right]u_{p,\sigma}, \tag{B13}$$

where $G_M = F_1 + F_2$ is the magnetic Sachs form factor determining the full magnetic moment $\mu = Q + \kappa = G_M(0)$. The first term is independent of the spin and is equal to the electromagnetic interaction of a scalar particle, which we omit as irrelevant to the discussion. With the use of (A3) and (B12), the spin-dependent interaction energy takes the form

$$E_{\mathrm{int,spin}} = iq_\nu A_\mu\left[eG_M\frac{\langle\!\langle\sigma^{\mu\nu}\rangle\!\rangle}{2m} - eF_3\frac{1}{2}\epsilon^{\mu\nu\rho\sigma}\frac{\langle\!\langle\sigma_{\rho\sigma}\rangle\!\rangle}{2m}\right]$$
$$= \frac{1}{2}\left(\frac{eG_M}{2m}F_{\mu\nu} - \frac{eF_3}{2m}\tilde{F}_{\mu\nu}\right)\langle\!\langle\sigma^{\mu\nu}\rangle\!\rangle. \tag{B14}$$

Neglecting all but the leading order in $O(|\vec{p}|,|\vec{p}'|)$, we only have to keep the spatial components $\langle\langle\sigma^{ij}\rangle\rangle$:

$$E_{\mathrm{int,spin}} = -\frac{eG_M}{2m}\vec{H}\cdot\hat{\Sigma} - \frac{eF_3}{2m}\vec{E}\cdot\hat{\Sigma}, \tag{B15}$$

where the unit spin vector $\hat{\Sigma} = \xi'^{\dagger}\vec{\sigma}\xi$, $|\hat{\Sigma}| = 1$. The coupling coefficients to the magnetic and electric fields in the above equation have to be identified with the magnetic and electric dipole moments, respectively:

$$\mu_N = G_M(0), \qquad d_N = F_3(0), \tag{B16}$$

both of which are expressed here in the particle magneton units $e/(2m)$.

Note that the above derivation could be repeated for the chirally rotated spinors and the nucleon-current vertex (13). It can be easily shown that the only change compared to Eq. (B15) would be that the magnetic and electric fields would couple to some orthogonal linear combinations of $\tilde{F}_{2,3}$, and that these combinations would reproduce F_2 and F_3 exactly in agreement with Eq. (25).

Finally, we note that if one uses the chirally rotated spinors to calculate the spatial matrix elements $\langle\!\langle\sigma^{ij}\rangle\!\rangle$, they are reduced by a factor of $\cos(2\alpha_5)$ while the timelike matrix elements $\langle\!\langle\sigma^{4k}\rangle\!\rangle$ become nonzero:

$$e^{2i\alpha_5\gamma_5}\sigma^{ij} = \cos(2\alpha_5)\sigma^{ij} + \sin(2\alpha_5)\epsilon^{ijk}\sigma^{4k},$$
$$e^{2i\alpha_5\gamma_5}\epsilon^{ijk}\sigma^{4k} = -\sin(2\alpha_5)\sigma^{ij} + \cos(2\alpha_5)\epsilon^{ijk}\sigma^{4k}. \tag{B17}$$

As we noted above, $\bar{u}_{p'}\sigma^{ij}u_p$ couples to the magnetic field, while $\bar{u}_{p'}\sigma^{4k}u_p$ couples to the electric field. This "mixing" of electric and magnetic fields compensates exactly the mixing in Eq. (25) induced by using the chirally rotated spinors $\bar{\tilde{u}}$, $\tilde{u}_p$ instead of the regular spinors $\bar{u}_{p'}$, u_p.

APPENDIX C: KINEMATIC COEFFICIENTS

In this appendix, we present expressions for the kinematic coefficients for form factors $F_{1,2,3}$ on a Euclidean lattice. We use two types of the polarization projectors: (1) spin-average

T^+ and (2) polarized $T^+_{S_z}$. Both projectors also select the upper (positive-parity) part of the nucleon spinors

$$T^+ = \left[\frac{1+\gamma^4}{2}\right]_{\mathcal{E}uc}, \qquad T^+_{S_z} = \left[\frac{1+\gamma^4}{2}(-i\gamma^1\gamma^2)\right]_{\mathcal{E}uc}. \tag{C1}$$

Form factor F_3 can be extracted from $\mu = 3$, 4 components of the vector current matrix elements between S_z-polarized nucleon states. Using handy notations for the positive-parity nucleon spinor matrices,

$$\mathcal{S} = -i\not{p}_{\mathcal{E}uc} + m, \qquad \mathcal{S}' = -i\not{p}'_{\mathcal{E}uc} + m, \tag{C2}$$

the form-factor expression for the $\not{C}\not{P}$ nucleon-current correlation function on a lattice $C^{\not{C}\not{P}}_{\mathrm{3pt}} = C^{\not{C}\not{P}}_{NJ^\mu\bar{N}}$ can be written as

$$\begin{aligned}
&\mathrm{Tr}[T_{\mathrm{pol}} C^{\not{C}\not{P}}_{NJ^\mu\bar{N}}(\vec{p}', t; \vec{q}, t_{\mathrm{op}})] \\
&= \frac{e^{-E'(t-t_{\mathrm{op}})-Et_{\mathrm{op}}}}{2E'2E}\mathrm{Tr}[e^{i\alpha_5\gamma_5} T e^{i\alpha_5\gamma_5}\mathcal{S}'\Gamma^\mu_{\mathcal{E}uc}(p', p)\mathcal{S}] \\
&= \frac{e^{-E'(t-t_{\mathrm{op}})-Et_{\mathrm{op}}}}{2E'2E}\mathrm{Tr}[(T + i\alpha_5\{\gamma_5, T\} \\
&\quad + O(\alpha_5{}^2))\mathcal{S}'\Gamma^\mu_{\mathcal{E}uc}(p', p)\mathcal{S}],
\end{aligned} \tag{C3}$$

where, assuming that the CP-odd interaction is small, we have expanded in the CP-odd mixing angle α_5.

Below, we quote formulas for contributions to the last line of Eq. (C3) computed for zero sink momentum $\vec{p}' = 0$:

$$\begin{aligned}
&\text{source } \vec{p} = -\vec{q}, \qquad E = \sqrt{m^2 + \vec{q}^2}, \\
&\text{sink } \vec{p}' = \vec{p} + \vec{q} = 0, \qquad E' = m,
\end{aligned}$$

with the nucleon spin projectors T^+ and $T^+_{S_z}$. The α_5-independent contribution is

$$\mathrm{Tr}[T^+\mathcal{S}'\Gamma^\mu_{\mathcal{E}uc}\mathcal{S}] = 4m^2\begin{pmatrix} iq_1/m & -i\tau q_1/m & 0 \\ iq_2/m & -i\tau q_2/m & 0 \\ iq_3/m & -i\tau q_3/m & 0 \\ 2(1+\tau) & -2\tau(1+\tau) & 0 \end{pmatrix}, \tag{C4}$$

$$\mathrm{Tr}[T^+_{S_z}\mathcal{S}'\Gamma^\mu_{\mathcal{E}uc}\mathcal{S}] = 4m^2\begin{pmatrix} -q_2/m & -q_2/m & q_1q_3/(2m^2) \\ q_1/m & q_1/m & q_2q_3/(2m^2) \\ 0 & 0 & q_3^2/(2m^2) \\ 0 & 0 & -i(1+\tau)q_3/m \end{pmatrix}, \tag{C5}$$

where the rows correspond to the Lorentz components $\mu = 1$, 2, 3, 4 and the columns correspond to the form factors $F_{1,2,3}$. We have also introduced the frequently used kinematic variable τ:

$$\tau \doteq \frac{Q^2}{4m^2} \overset{\vec{p}'=0}{\equiv} \frac{E-m}{2m}. \tag{C6}$$

The coefficients of the contributions $\propto\alpha_5$ are

$$\mathrm{Tr}[\{\gamma_5, T^+\}\mathcal{S}'\Gamma^\mu_{\mathcal{E}uc}\mathcal{S}] = 4m^2\begin{pmatrix} 0 & 0 & -\tau q_1/m \\ 0 & 0 & -\tau q_2/m \\ 0 & 0 & -\tau q_3/m \\ 0 & 0 & 2i\tau(1+\tau) \end{pmatrix}, \tag{C7}$$

$$\begin{aligned}
&\mathrm{Tr}[\{\gamma_5, T^+_{S_z}\}\mathcal{S}'\Gamma^\mu_{\mathcal{E}uc}\mathcal{S}] \\
&= 4m^2\begin{pmatrix} 0 & iq_1q_3/(2m^2) & 0 \\ 0 & iq_2q_3/(2m^2) & 0 \\ -2i\tau & -2i\tau + iq_3^2/(2m^2) & 0 \\ -q_3/m & \tau q_3/m & 0 \end{pmatrix}.
\end{aligned} \tag{C8}$$

Up to order $O(\alpha_5)$, the $\not{C}\not{P}$ nucleon correlation functions are[7]

$$\mathrm{Tr}[T^+ C^{\not{C}\not{P}}_{NJ^3\bar{N}}] = \mathcal{K}\left[i\frac{q_3}{m}G_E + O(\alpha_5{}^2)\right], \tag{C9}$$

$$\mathrm{Tr}[T^+ C^{\not{C}\not{P}}_{NJ^4\bar{N}}] = \mathcal{K}[2(1+\tau)G_E + O(\alpha_5{}^2)], \tag{C10}$$

$$\begin{aligned}
\mathrm{Tr}[T^+_{S_z} C^{\not{C}\not{P}}_{NJ^3\bar{N}}] = \mathcal{K}\Bigg[&2\tau\alpha_5 G_M - \alpha_5\frac{q_3^2}{2m^2}F_2 \\
&+ \frac{q_3^2}{2m^2}F_3 + O(\alpha_5{}^2)\Bigg],
\end{aligned} \tag{C11}$$

$$\begin{aligned}
\mathrm{Tr}[T^+_{S_z} C^{\not{C}\not{P}}_{NJ^4\bar{N}}] = \mathcal{K}\Bigg[&-i\alpha_5\frac{q_3}{m}G_E \\
&- i(1+\tau)\frac{q_3}{m}F_3 + O(\alpha_5{}^2)\Bigg],
\end{aligned} \tag{C12}$$

where $G_E = F_1 - \tau F_2$ is the electric and $G_M = F_1 + F_2$ is the magnetic Sachs form factor, and

$$\mathcal{K} = \frac{m}{E}e^{-E'(t_{\mathrm{sep}}-t_{\mathrm{op}})-Et_{\mathrm{op}}} \tag{C13}$$

is the time dependence combined with kinematic factors. In the analysis of the $C_{NJ\bar{N}}/C_{N\bar{N}}$ ratios (60), the exponential time dependence is canceled, and the kinematic coefficients have to be modified to take into account the traces of the nucleon two-point functions:

$$\mathcal{K}_{\mathcal{R}} = \frac{m}{\sqrt{2E(m+E)}}. \tag{C14}$$

In addition, we evaluate the extra contributions to the kinematic coefficients $\sim\alpha_5\{\gamma_5, \Gamma^\mu_{\mathcal{E}uc}\}$ that come from spurious mixing of $F_{2,3}$:

[7] Note that both α_5 and F_3 are proportional to the CP-odd perturbation; therefore, we consider $F_3 = O(\alpha_5)$ and drop terms $\alpha_5 F_3$ and higher.

$$\mathrm{Tr}[T^+\mathcal{S}'\{\gamma_5,\Gamma^\mu_{\mathcal{E}uc}\}\mathcal{S}] = 4m^2\begin{pmatrix} 0 & 0 & 2\tau q_1/m \\ 0 & 0 & 2\tau q_2/m \\ 0 & 0 & 2\tau q_3/m \\ 0 & 0 & -4i\tau(1+\tau) \end{pmatrix}, \tag{C15}$$

$$\mathrm{Tr}[T^+_{S_z}\mathcal{S}'\{\gamma_5,\Gamma^\mu_{\mathcal{E}uc}\}\mathcal{S}] = 4m^2\begin{pmatrix} 0 & -iq_1q_3/m^2 & -2iq_2/m \\ 0 & -iq_2q_3/m^2 & 2iq_1/m \\ 0 & -iq_3^2/m^2 & 0 \\ 0 & -2(1+\tau)q_3/m & 0 \end{pmatrix}, \tag{C16}$$

which in Refs. [5–11] contributes to the polarized nucleon-current correlators as

$$\delta\mathrm{Tr}[T^+_{S_z}C^{\not{C}\not{P}}_{NJ^3\bar{N}}] \stackrel{?}{=} \mathcal{K}\left[\alpha_5\frac{q_3^2}{m^2}F_2 + O(\alpha_5{}^2)\right], \tag{C17}$$

$$\delta\mathrm{Tr}[T^+_{S_z}C^{\not{C}\not{P}}_{NJ^4\bar{N}}] \stackrel{?}{=} \mathcal{K}\left[-2i\alpha_5(1+\tau)\frac{q_3}{m}F_2 + O(\alpha_5{}^2)\right]. \tag{C18}$$

If the terms (C17) and (C18) are erroneously added to the kinematic coefficients (C11) and (C12), analysis of the same lattice correlation functions will result in incorrect values of EDFF, $\tilde{F}_3 = F_3 - 2\alpha_5 F_2$, in full agreement with Eq. (25).

[1] J. Engel, M. J. Ramsey-Musolf, and U. van Kolck, Prog. Part. Nucl. Phys. **71**, 21 (2013).
[2] S. Aoki and A. Gocksch, Phys. Rev. Lett. **63**, 1125 (1989); **65**, 1172(E) (1990).
[3] E. Shintani, S. Aoki, N. Ishizuka, K. Kanaya, Y. Kikukawa, Y. Kuramashi, M. Okawa, A. Ukawa, and T. Yoshié, Phys. Rev. D **75**, 034507 (2007).
[4] E. Shintani, S. Aoki, and Y. Kuramashi, Phys. Rev. D **78**, 014503 (2008).
[5] E. Shintani, S. Aoki, N. Ishizuka, K. Kanaya, Y. Kikukawa, Y. Kuramashi, M. Okawa, Y. Taniguchi, A. Ukawa, and T. Yoshié, Phys. Rev. D **72**, 014504 (2005).
[6] F. Berruto, T. Blum, K. Orginos, and A. Soni, Phys. Rev. D **73**, 054509 (2006).
[7] R. Horsley *et al.*, arXiv:0808.1428.
[8] F. K. Guo, R. Horsley, U.-G. Meißner, Y. Nakamura, H. Perlt, P. E. L. Rakow, G. Schierholz, A. Schiller, and J. M. Zanotti, Phys. Rev. Lett. **115**, 062001 (2015).
[9] A. Shindler, T. Luu, and J. de Vries, Phys. Rev. D **92**, 094518 (2015).
[10] C. Alexandrou, A. Athenodorou, M. Constantinou, K. Hadjiyiannakou, K. Jansen, G. Koutsou, K. Ottnad, and M. Petschlies, Phys. Rev. D **93**, 074503 (2016).
[11] E. Shintani, T. Blum, T. Izubuchi, and A. Soni, Phys. Rev. D **93**, 094503 (2016).
[12] R. J. Crewther, P. Di Vecchia, G. Veneziano, and E. Witten, Phys. Lett. **88B**, 123 (1979).
[13] A. Pich and E. de Rafael, Nucl. Phys. **B367**, 313 (1991).
[14] M. Pospelov and A. Ritz, Phys. Rev. Lett. **83**, 2526 (1999).
[15] M. Pospelov and A. Ritz, Phys. Rev. D **63**, 073015 (2001).
[16] J. Hisano, J. Y. Lee, N. Nagata, and Y. Shimizu, Phys. Rev. D **85**, 114044 (2012).
[17] B. Borasoy, Phys. Rev. D **61**, 114017 (2000).
[18] E. Mereghetti, J. de Vries, W. H. Hockings, C. M. Maekawa, and U. van Kolck, Phys. Lett. B **696**, 97 (2011).
[19] T. Bhattacharya, V. Cirigliano, R. Gupta, H.-W. Lin, and B. Yoon, Phys. Rev. Lett. **115**, 212002 (2015).
[20] T. Bhattacharya, V. Cirigliano, R. Gupta, E. Mereghetti, and B. Yoon, *Proc. Sci.*, LATTICE2015 (2015) 238.
[21] T. Bhattacharya, V. Cirigliano, R. Gupta, and B. Yoon, *Proc. Sci.*, LATTICE2015 (2016) 225.
[22] W. Detmold, B. C. Tiburzi, and A. Walker-Loud, Phys. Rev. D **79**, 094505 (2009).
[23] C. Itsykson and J.-B. Zuber, *Quantum Field Theory* (McGraw-Hill, New York, 1984) Chap. 3.4.4.
[24] W. Detmold, B. C. Tiburzi, and A. Walker-Loud, Phys. Rev. D **81**, 054502 (2010).
[25] T. Blum *et al.*, Phys. Rev. D **84**, 114503 (2011).
[26] Y. Aoki *et al.*, Phys. Rev. D **83**, 074508 (2011).
[27] T. Blum *et al.*, Phys. Rev. D **93**, 074505 (2016).
[28] E. Shintani, R. Arthur, T. Blum, T. Izubuchi, C. Jung, and C. Lehner, Phys. Rev. D **91**, 114511 (2015).
[29] R. Brower, H. Neff, and K. Orginos, Nucl. Phys. B, Proc. Suppl. **153**, 191 (2006).
[30] S. Syritsyn *et al.*, Phys. Rev. D **81**, 034507 (2010).
[31] C. Allton *et al.*, Phys. Rev. D **76**, 014504 (2007).
[32] T. Bhattacharya, V. Cirigliano, R. Gupta, E. Mereghetti, and B. Yoon, Phys. Rev. D **92**, 114026 (2015).
[33] A. Abdel-Rehim *et al.*, *Proc. Sci.*, LATTICE2014 (2015) 148.
[34] E. Shintani (private communication).
[35] P. E. Shanahan, R. Horsley, Y. Nakamura, D. Pleiter, P. E. L. Rakow, G. Schierholz, H. Stüben, A. W. Thomas, R. D. Young, and J. M. Zanotti, Phys. Rev. D **89**, 074511 (2014).
[36] F.-K. Guo and U.-G. Meissner, J. High Energy Phys. 12 (2012) 097.
[37] C. Bouchard, C. C. Chang, T. Kurth, K. Orginos, and A. Walker-Loud, arXiv:1612.06963.
[38] A. S. Gambhir *et al.*, *Proc. Sci.*, LATTICE2016 (2016) 265.
[39] A. Pochinsky, Qlua software, https://usqcd.lns.mit.edu/qlua.
[40] L. Landau and E. Lifshitz, *The Classical Theory of Fields*, 4th ed., Course of Theoretical Physics Vol. 2 (Butterworth-Heinemann, Oxford, England, 1980).